Accepted Manuscript

Design, synthesis and biological evaluation of novel benzothiadiazine derivatives as potent PI3Kδ-selective inhibitors for treating B-cell-mediated malignancies

Xiaodong Ma, Jun Wei, Chang Wang, Dongyan Gu, Yongzhou Hu, Rong Sheng

PII: S0223-5234(19)30216-8

DOI: https://doi.org/10.1016/j.ejmech.2019.03.005

Reference: EJMECH 11175

To appear in: *European Journal of Medicinal Chemistry*

Received Date: 11 January 2019

Revised Date: 27 February 2019

Accepted Date: 2 March 2019

Please cite this article as: X. Ma, J. Wei, C. Wang, D. Gu, Y. Hu, R. Sheng, Design, synthesis and biological evaluation of novel benzothiadiazine derivatives as potent PI3Kδ-selective inhibitors for treating B-cell-mediated malignancies, *European Journal of Medicinal Chemistry* (2019), doi: https://doi.org/10.1016/j.ejmech.2019.03.005.

Graphical abstract

Design, Synthesis and Biological Evaluation of Novel Benzothiadiazine Derivatives as Potent PI3Kδ-selective Inhibitors for Treating B-cell-mediated Malignancies

Xiaodong Ma [a, b, c], Jun Wei [a], Chang Wang [a], Dongyan Gu [a], Yongzhou Hu [a], Rong Sheng [a, *]

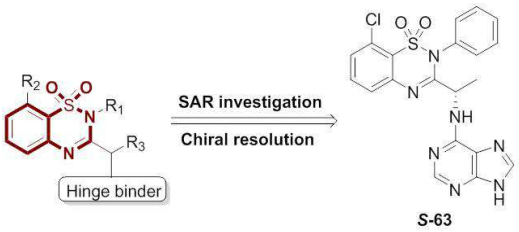

- Absolute configuration determined by X-ray single crystal diffraction
- PI3Kδ IC_{50}: 4.6 nM; SU-DHL-6 GI_{50} 33.2 nM
- Excellent PI3Kδ specificity
- Acceptable oral bioavailability (F% = 29.2)

Design, Synthesis and Biological Evaluation of Novel Benzothiadiazine Derivatives as Potent PI3Kδ-selective Inhibitors for Treating B-cell-mediated Malignancies

Xiaodong Ma [a, b, c], Jun Wei [a], Chang Wang [a], Dongyan Gu [a], Yongzhou Hu [a], Rong Sheng [a, *]

a. ZJU-ENS Joint Laboratory of Medicinal Chemistry, Zhejiang Province Key Laboratory of Anti-Cancer Drug Research, College of Pharmaceutical Sciences, Zhejiang University, Hangzhou 310058, China

b. School of Pharmacy, Anhui University of Chinese Medicine, Hefei 230031, China

c. Department of Medicinal Chemistry, Anhui Academy of Chinese Medicine, Hefei 230031, China

Abstract: A series of 24 benzothiadiazine derivatives with structural novelty were designed, synthesized and biologically evaluated as PI3Kδ-selective inhibitors. As a consequence of the structure-activity relationship (SAR) study, compounds **63** and **71** were identified with single-digit nanomolar IC_{50} values against PI3Kδ and submicromolar GI_{50} values against human malignant B-cell line SU-DHL-6. Furthermore, chiral resolution of the key amine intermediate of these two compounds was performed to achieve corresponding enantiomers. In subsequent biological evaluation, ***S*-63** (IC_{50}: 4.6 nM) and ***S*-71** (IC_{50}: below 0.32 nM) demonstrated comparable and superior PI3Kδ inhibitory activity, respectively, to that of idelalisib. Additionally, both ***S*-63** (GI_{50}: 33.2 nM) and ***S*-71** (GI_{50}: 15.9 nM) exerted enhanced anti-proliferative activity against the SU-DHL-6 cell line than that of idelalisib. Moreover, both ***S*-63** and ***S*-71** exhibited excellent PI3Kδ selectivity. In the further *in vivo* pharmacokinetic (PK) study, ***S*-63** displayed a good plasma exposure and an acceptable oral bioavailability of 29.2%. By virtue of its biological performance, ***S*-63** merits further development as a potential therapeutic agent for battling B-cell-mediated malignancies.

Key words: Benzothiadiazine derivatives; PI3Kδ-selective inhibitors; SAR; Chiral resolution; PK study

* Corresponding author: Rong Sheng

ZJU-ENS Joint Laboratory of Medicinal Chemistry, Zhejiang Province Key Laboratory of Anti-Cancer Drug Research, College of Pharmaceutical Sciences, Zhejiang University, Hangzhou 310058, China

E-mail: shengr@zju.edu.cn

1. Introduction

Aberrant phosphoinositide 3-kinase (PI3K) signaling is implicated in a myriad of pathological conditions [1-5]. PI3K, the lipid kinase transforming phosphatidylinositol 4, 5-bisphosphate (PIP_2) to the second messenger phosphatidylinositol 3, 4, 5-trisphosphate (PIP_3), comprises several classes, among which class I PI3Ks have been widely accepted as targets for battling human malignancies [6-8]. Owing to the differentiation in the catalytic subunit and biological function, Class I PI3Ks can be further divided into four highly homologous subtypes, PI3Kα, PI3Kβ, PI3Kγ and PI3Kδ [9].

Predominantly enriched in leukocytes, and essential for B-cell proliferation and function, PI3Kδ provides a unique opportunity for therapeutic intervention in B-cell-mediated malignancies, autoimmune disorders, and inflammatory diseases [10-13]. In comparison, PI3Kα and PI3Kβ are ubiquitously expressed and vital for embryonic development, insulin action, as well as platelet aggregation [9, 14-16]. Considering these characteristics, the application of pan-class I PI3K inhibitors for treating leukocyte-mediated conditions may be compromised by limited tolerability due to the concomitant suppression of other subtypes irrelevant to disease initiation and progression [17, 18]. Hence, the past decade has witnessed an increasing investment in PI3Kδ-selective inhibitors specifically ablating PI3Kδ signaling without interfering with the biological function of the other three class I PI3K isoforms [19-24].

Idelalisib (Zydelig) **1** is the first-in-class PI3Kδ-selective inhibitor approved for treating chronic lymphocytic leukemia (CLL), follicular lymphoma (FL), and small lymphocytic lymphoma (SLL) in 2014 [25, 26]. Duvelisib **2**, a δ-weighted PI3Kδ/γ dual inhibitor [27], has also been approved recently for curing hematopoietic malignancies. Several other candidates, as exemplified by acalisib **3**, AMG-319 **4**, tenalisib **5** and umbralisib **6** (https://www.pharmacodia.com/cn), have progressed to clinical trials as remedies for B or T cell-related malignancies (**Figure 1**). With respect to the binding mode, these advanced PI3Kδ inhibitors may be defined as ATP-competitive allosteric inhibitors and are capable of inducing a hydrophobic selectivity pocket between residues Trp760 and Met752, which is not present in the apo structure of the enzyme [28, 29].

Despite differentiated chemical structures, these allosteric inhibitors, also termed as the propeller-shaped inhibitors, harbor approximately the same pharmacophore, featuring a bicyclic heteroaromatic core, a six-membered aryl group directly attached to it, as well as a hinge binder (HB) tethered to it *via* a short spacer [30] (**Figure 1**). Among these, the six-membered aryl moiety and HB

assume a perpendicular conformation to the heteroaromatic core that is embedded in the selectivity pocket. The spacer between the bicyclic heteroaromatic core and HB, commonly containing an amino linker and a chiral carbon, is vital for inducing the specificity pocket. In addition to the PI3Kδ inhibitors characterized by this pharmacophore, recent medicinal chemistry efforts have also culminated in propeller-shaped inhibitors with nonfused aromatic core, and nonpropeller-shaped inhibitors [31].

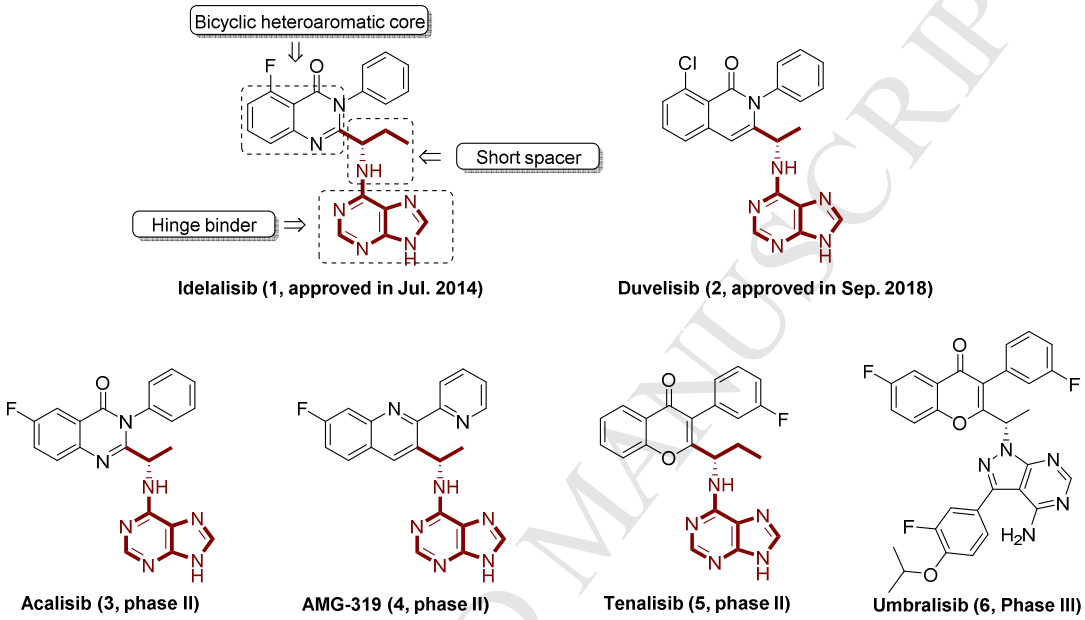

Figure 1. The approved or clinically investigated PI3Kδ-selective inhibitors.

Built upon our insight into the typical propeller-shaped PI3Kδ-selective inhibitors, especially the successful exploration of **2**, **4** and **5** *via* bioisosterism, we envisioned that replacement of quinazolinone of idelalisib with the benzothiadiazine template may be a feasible approach to obtaining novel PI3Kδ-selective inhibitors (**Figure 2**). To explore the structure-activity relationships (SARs) of these benzothiadiazines, different R_1, R_2 and R_3 substituents were investigated to obtain optimal moieties. Also, for some compounds, the aminopurine was replaced by its ring-opening surrogate 4, 6-diamino-5-carbonitrile pyrimidine, or reversed with its *N*9 tethered to the chiral carbon. Through careful modification on *N*-2 phenyl moiety, C-8 replacement, C-3 short spacer, and hinge binder, both compounds **63** and **71** were identified with attractive PI3Kδ inhibitory activity and anti-proliferative efficacy. In addition, chiral resolution of the key amine intermediate towards the preparation of representative compounds (**63** and **71**) was performed to pave the way for revealing the impact of absolute configuration on PI3Kδ inhibitory activity and specificity. Based on the *in vitro* biological evaluation, ***S*-63**, the most promising benzothiadiazine derivative throughout the series, was further

investigated for *in vivo* PK profiles. We herein communicate our recent efforts leading to a novel structural series of benzothiadiazine derivatives as PI3Kδ-selective inhibitors.

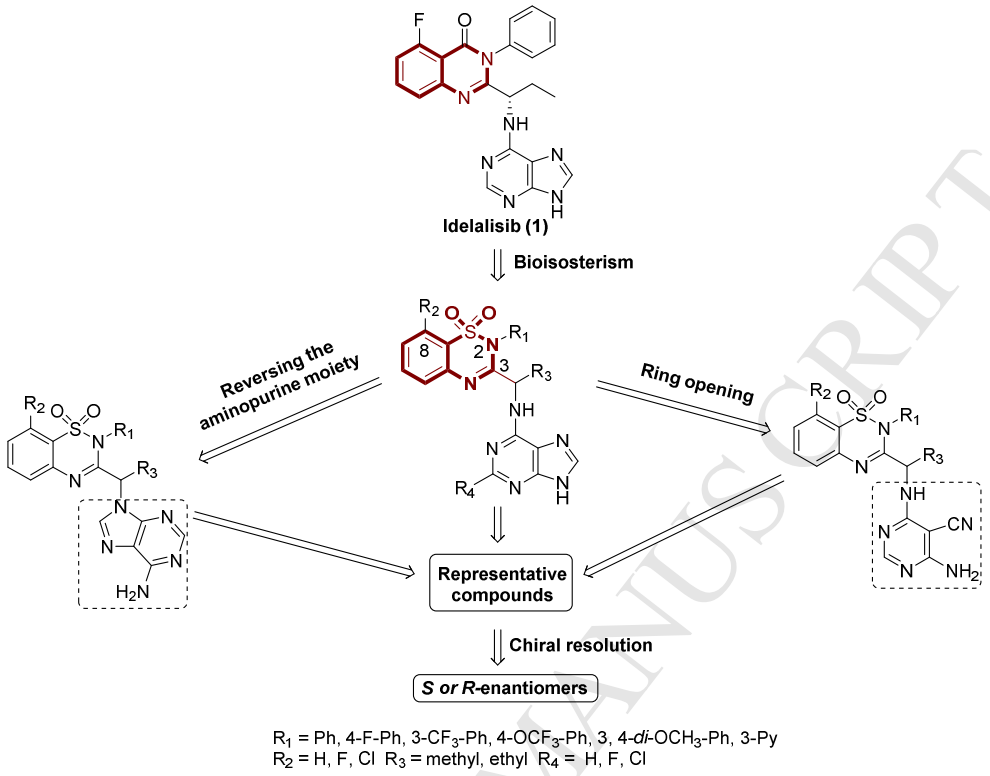

Figure 2. The design rationale of target benzothiadiazine derivatives.

2. Results and Discussion

2.1. Chemistry

The synthetic route to target benzothiadiazine derivatives is displayed in **Scheme 1**. 1, 2-difluoro-3-nitrobenzene **7** or 1, 2-dichloro-3-nitrobenzene **8** was converted into corresponding benzenesulfonyl chloride **9** or **10**, respectively, according to a reported procedure [32]. The resulting products or 2-nitrobenzenesulfonyl chloride **11** were subsequently condensed with various aromatic amines to afford sulfonamides **12−19**. The nitro moiety of the sulfonamides was then reduced by $NaBH_4$, and the produced amines were converted to C-3 alkyl substituted benzothiadiazines **20−31** after condensation with orthoester and intramolecular cyclization [33]. Next, *α*-bromination of the derived products yielded **32−43** [34, 35], which were subjected to a two-step Gabriel synthesis to generate the key amine intermediates **44−54**. Ultimately, **44−54** reacted with 6-chloro-9*H*-purine, 6-chloro-2-fluoro-9*H*-purine, 2,6-dichloro-9*H*-purine or 4-amino-6-chloropyrimidine-5-carbonitrile to produce **55−72** as the target compounds [18, 21, 36]. Additionally, the treatment of bromides **32−34**, **37**, **39** and **40** with adenine in the presence of K_2CO_3 gernerated target compounds **73−78**.

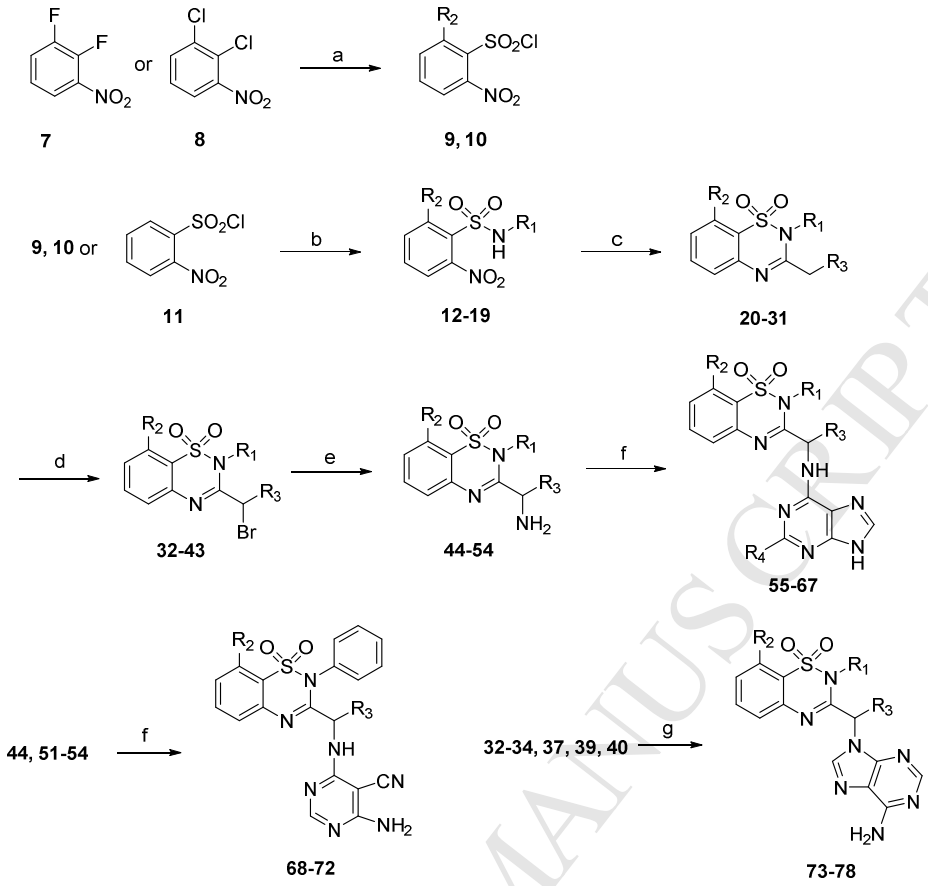

9 R_2=F
10 R_2=Cl
12 R_1=Ph, R_2=H
13 R_1=4-F-Ph, R_2=H
14 R_1=3-CF_3-Ph, R_2=H
15 R_1=4-OCF_3-Ph, R_2=H
16 R_1=3, 4-*di*-OCH_3-Ph, R_2=H
17 R_1=3-Py, R_2=H
18 R_1=Ph, R_2=F
19 R_1=Ph, R_2=Cl

20, 32, 44, 55 R_1=Ph, R_2=H, R_3=Me, R_4=H
21, 33, 45, 56 R_1=4-F-Ph, R_2=H, R_3=Me, R_4=H
22, 34 R_1=4-F-Ph, R_2=H, R_3=Et
23, 35, 46, 57 R_1=3-CF_3-Ph, R_2=H, R_3=Me, R_4=H
24, 36, 47, 58 R_1=3-CF_3-Ph, R_2=H, R_3=Et , R_4=H
25, 37, 48, 59 R_1=4-OCF_3-Ph, R_2=H, R_3=Et, R_4=H
26, 38, 49, 60 R_1=3, 4-*di*-OCH_3-Ph, R_2=H, R_3=Et, R_4=H
27, 39, 50, 61 R_1=3-Py, R_2=H, R_3=Me, R_4=H
28, 40, 51 R_1=Ph, R_2=F, R_3=Me
29, 41, 52, 62 R_1=Ph, R_2=F, R_3=Et, R_4=H
30, 42, 53, 63 R_1=Ph, R_2=Cl, R_3=Me, R_4=H
31, 43, 54, 64 R_1=Ph, R_2=Cl, R_3=Et, R_4=H

65 R_1=Ph, R_2=H, R_3=Me, R_4=F
66 R_1=Ph, R_2=H, R_3=Me, R_4=Cl
67 R_1=Ph, R_2=F, R_3=Et, R_4=F
68 R_2=H, R_3=Me
69 R_2=F, R_3=Me
70 R_2=F, R_3=Et
71 R_2=Cl, R_3=Me
72 R_2=Cl, R_3=Et

73 R_1=Ph, R_2=H, R_3=Me
74 R_1=4-F-Ph, R_2=H,R_3=Me
75 R_1=4-F-Ph, R_2=H, R_3=Et
76 R_1=4-OCF_3-Ph, R_2=H, R_3=Et
77 R_1=3-Py, R_2=H, R_3=Me
78 R_1=Ph, R_2=F, R_3=Me

Scheme 1. Reagents and conditions: (a) (1) benzyl mercaptan, K_2CO_3, DMF, rt; (2) Cl_2, DCM/H_2O, 0 °C; (b) corresponding aromatic amine, pyridine, DCM, 0 °C to rt; (c) (1) $NaBH_4$, $NiCl_2$ (hexahydrate), MeOH/DCM, 0 °C to rt; (2) corresponding orthoester, 130 °C, N_2; (3) Ph_2O, 250 °C, N_2 (As for **30** and **31**, intramolecular cyclization occurred during the treatment with orthoester, and this step was omitted); (d) Br_2, AcONa, AcOH, 40 °C; (e) (1) phthalimide, K_2CO_3, DMF, 40 °C; (2) hydrazine hydrate (85%), EtOH, 80 °C, N_2; (f) 6-chloro-9*H*-purine, 6-chloro-2-fluoro-9*H*-purine, 2,6-dichloro-9*H*-purine or 4-amino-6-chloropyrimidine-5-carbonitrile, DIPEA, *t*-BuOH, 80 °C, N_2; (g) adenine, K_2CO_3, DMF, rt.

2.2. SAR Investigation

According to the design rationale summarized in **Figure 2**, 24 benzothiadiazines were prepared and biologically evaluated for the PI3Kδ inhibitory activity. The experimental data of compounds bearing aminopurine as HB and those bearing 4, 6-diamino-5-carbonitrile pyrimidine or reversed aminopurine as HB are displayed in **Table 1** and **Table 2**, respectively. Among them, 9 compounds, including **63**−**65**, **68**, **69**, **71**−**73** and **78**, exhibited potent PI3Kδ inhibitory activity with IC_{50} values below 100 nM. In particular, the purine derivative **63** and 4, 6-diamino-5-carbonitrile pyrimidine derivative **71**, both with C-8 chloro and C-3 ethyl substitution, exerted remarkable PI3Kδ inhibitory activity with respective IC_{50} values of 9.8 and 3.2 nM.

Table 1. PI3Kδ inhibitory activity of target compounds bearing aminopurine as HB.

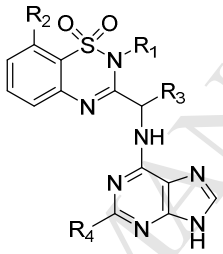

Cpd.	R_1	R_2	R_3	R_4	PI3Kδ (IC_{50}, nM)
55	Ph	H	Me	H	344
56	4-F-Ph	H	Me	H	1999
57	3-CF_3-Ph	H	Me	H	>3000
58	3-CF_3-Ph	H	Et	H	>3000
59	4-OCF_3-Ph	H	Et	H	>3000
60	3, 4-*di*-OCH_3-Ph	H	Et	H	>3000
61	3-Py	H	Me	H	921
62	Ph	F	Et	H	>3000
63	Ph	Cl	Me	H	9.8
64	Ph	Cl	Et	H	81
65	Ph	H	Me	F	92
66	Ph	H	Me	Cl	1202
67	Ph	F	Et	F	383
PI-103					14

Table 2. PI3Kδ inhibitory activity of target compounds bearing 4, 6-diamino-5-carbonitrile pyrimidine or reversed aminopurine as HB.

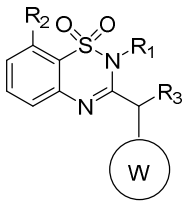

Cpd.	R_1	R_2	R_3	W	PI3Kδ (IC_{50}, nM)
68	Ph	H	Me	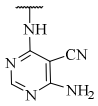	15
69	Ph	F	Me	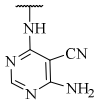	35
70	Ph	F	Et	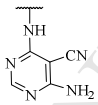	141
71	Ph	Cl	Me	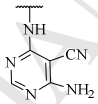	3.2
72	Ph	Cl	Et	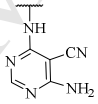	12
73	Ph	H	Me	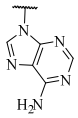	68
74	4-F-Ph	H	Me	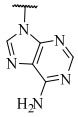	628
75	4-F-Ph	H	Et	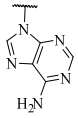	>3000
76	4-OCF_3-Ph	H	Et	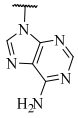	>3000
77	3-Py	H	Me	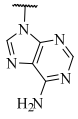	623
78	Ph	F	Me	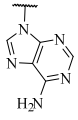	54
PI-103					14

From the biological data presented in **Table 1** and **2**, some valuable SARs can be deduced. Firstly, the *N*-2 phenyl moiety was optimum and substitution at the phenyl was detrimental to PI3Kδ inhibitory activity. In addition, replacing the *N*-2 phenyl moiety with pyridinyl weakened the enzymatic activity by approximately 3-fold (**61** versus **55**). When comparing **58** (IC_{50} > 3000 nM) to **59** (IC_{50} > 3000 nM) or **60** (IC_{50} > 3000 nM), it became evident that neither the 4-OCF_3 nor 3, 4-*di*-OCH_3 substitution boosted PI3Kδ inhibitory activity. Secondly, the introduction of a chloro-substituent at the C-8 position significantly improved PI3Kδ inhibitory activity. As for compounds with aminopurine as HB, C-8 chlorinated compound **63** (IC_{50} = 9.8 nM) was 35-fold more potent than its C-8 unsubstituted counterpart **55**, and C-8 chlorinated compound **64** (IC_{50} = 81 nM) was over 35-fold more active than C-8 fluorinated counterpart **62** (IC_{50} > 3000 nM). Similar results can also be observed for benzothiadiazines with 4, 6-diamino-5-carbonitrile pyrimidine as HB, e.g. **71** versus **68**, **71** versus **69**, and **72** versus **70**. Thirdly, HB had an important impact on PI3Kδ inhibitory activity. Replacing aminopurine with 4, 6-diamino-5-carbonitrile pyrimidine can dramatically improve PI3Kδ inhibitory activity, as illustrated by **68** versus **55**, **70** versus **62**, **71** versus **63**, and **72** versus **64**. The reversion of the aminopurine also enhanced PI3Kδ inhibitory activity, as demonstrated by **73** versus **55**, **74** versus **56**, and **77** versus **61**. Finally, compounds with a C-3 ethyl substituent were superior to their counterparts with a C-3 propyl substituent in PI3Kδ inhibitory activity, as shown by **63** versus **64**, **69** versus **70**, and **71** versus **72**.

Table 3. The anti-proliferative activity of selected compounds against SU-DHL-6 cell line.

Cpd.	SU-DHL-6 (GI_{50}, nM)	Cpd.	SU-DHL-6 (GI_{50}, nM)
63	770	**71**	187
64	2193	**72**	1675
65	4689	**73**	23147
68	3501	**78**	7203
69	1217	**Paclitaxel**	7.9
70	10511		

Compounds with PI3Kδ IC_{50} values below 200 nM were evaluated for their anti-proliferative activity against the human malignant B-cell line SU-DHL-6. In general, over half of them exhibited favorable

anti-proliferative efficacy with GI_{50} values ranging from low micromolar to submicromolar level, and the cellular activity was consistent with the enzymatic activity (**Table 3**). Compounds **63** and **71**, the two most potent PI3Kδ inhibitors throughout this series, also exerted remarkable anti-proliferative efficacy with respective GI_{50} values of 770 and 187 nM against the SU-DHL-6 cell line.

2.3. Chiral Resolution

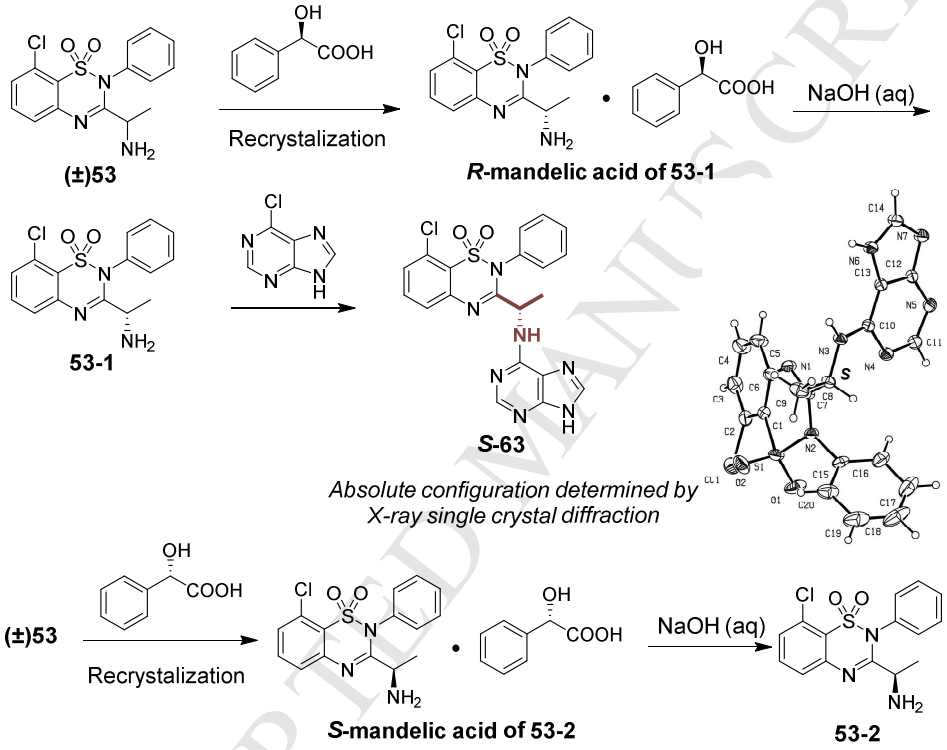

Figure 3. The chiral resolution of the key amine intermediate **53** and the result for X-ray single crystal diffraction of ***S*-63**.

Upon SAR investigation stated above, two benzothiadiazine derivatives **63** and **71** were identified with promising *in vitro* potency, both characterized by single-digit nanomolar PI3Kδ inhibitory activity and submicromolar anti-proliferative efficacy. Therefore, we subsequently undertook the chiral resolution of **53**, the key amine intermediate towards the preparation of compounds **63** and **71**, which would pave the way to reveal how the absolute configuration affected PI3Kδ inhibitory activity and subtype specificity (**Figure 3**). Through our investigation on different chiral resolving reagents, *S* or *R*-mandelic acid was identified to be optimum. Both the *R*-mandelic acid salt of **53-1** and *S*-mandelic

acid salt of **53-2** were attained in high *de* value (over 95%) after recrystallization from ethyl acetate (EA). After basifying the *R*-mandelic acid salt of **53-1**, the free amine was converted into the corresponding purine derivative ***S*-63**, the absolute configuration of which was determined *via* X-ray single crystal diffraction. Accordingly, the absolute configurations of **53-1** and **53-2** were determined as *S* and *R*, respectively. On the basis of this, we prepared ***R*-63**, ***S*-71** and ***R*-71** for further biological evaluation.

2.4. In Vitro Activity and Subtype Selectivity of Optically Pure Compounds

Table 4. *In vitro* activity of the optically pure compounds.

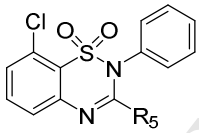

Cpd.	R_5	PI3Kδ (IC_{50}, nM) [a]	SU-DHL-6 (GI_{50}, nM) [a]
***S*-63**	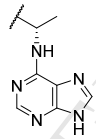	4.6	33.2
***R*-63**	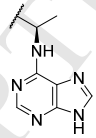	62	190
***S*-71**	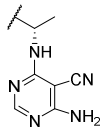	＜0.32	15.9
***R*-71**	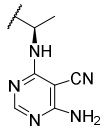	7.0	70.3
Idelalisib		1.8	124

a. The data were obtained from separated experiment from corresponding one performed for the racemates.

The successful resolution of the key amine intermediate **53** prompted us to investigate the PI3Kδ

inhibitory potency and subtype specificity of the optically pure compounds, including ***S*-63**, ***R*-63**, ***S*-71** and ***R*-71** (**Table 4**). Consequently, ***S*-63** and ***R*-71**, with respective IC_{50} values of 4.6 and 7.0 nM, exhibited comparable PI3Kδ inhibitory activity to that of idelalisib. In particular, ***S*-71** demonstrated potent PI3Kδ inhibitory activity with IC_{50} value below 0.32 nM, which was superior to that of idelalisib. Importantly, the impact of absolute configuration on enzymatic activity was clearly observed according to the obtained biological data, and the *S*-enantiomers (***S*-63** and ***S*-71**) displayed dramatically improved enzymatic potency compared to that of corresponding *R*-enantiomers (***R*-63** and ***R*-71**). In addition to the favorable enzymatic activity, both ***S*-63** and ***S*-71**, with respective GI_{50} values of 33.2 and 15.9 nM, exhibited enhanced anti-proliferative activity than that of idelalisib.

The absolute configuration also had a considerable influence on subtype specificity, as illustrated by the superior PI3Kδ specificity of ***S*-63** and ***S*-71** to that of the corresponding enantiomers ***R*-63** and ***R*-71** over the other class I PI3K subtypes (**Table 5**). Among them, ***S*-63** exhibited comparable δ-subtype selectivity to that of idelalisib, while ***S*-71** displayed a more favorable specificity.

Table 5. Subtype specificity data of optically pure compounds.

Kinases	***S*-63** (IC_{50}, nM)	***R*-63** (IC_{50}, nM)	***S*-71** (IC_{50}, nM)	***R*-71** (IC_{50}, nM)	**Idelalisib** (IC_{50}, nM)
PI3Kδ	4.6	62	< 0.32	7.0	1.8
PI3Kα	3637 (**791-fold**)[a]	>5000 (**>81-fold**)[a]	996 (**>3113-fold**)[a]	>5000 (**>714-fold**)[a]	2164 (**1202-fold**)[a]
PI3Kβ	766 (**167-fold**)[a]	3990 (**64-fold**)[a]	55 (**>172-fold**)[a]	169 (**24-fold**)[a]	154 (**85-fold**)[a]
PI3Kγ	156 (**34-fold**)[a]	1905 (**31-fold**)[a]	100 (**>313-fold**)[a]	112 (**16-fold**)[a]	63 (**35-fold**)[a]

a. Selectivity fold

2.5. Pharmacokinetics (PKs)

By virtue of the favorable PI3Kδ inhibitory activity and specificity, ***S*-63** was selected for further PK evaluation in Sprague−Dawley (SD) Rats with idelalisib used as the reference. Despite its better PI3Kδ

inhibitory activity and specificity, ***S*-71** exhibited a remarkably lower AUC value than that of ***S*-63** in the preliminary PK evaluation (Data not shown) and was not investigated extensively. As shown in **Table 6**, ***S*-63** displayed a favorable plasma exposure (AUC_{0-t} = 2009±993 h ng/mL) and an acceptable oral bioavailability (F% = 29.2±14.7). Moreover, the clearance, volume distribution, and elimination half-life were comparable to those of idelalisib.

Table 6. The PK property of selected compound ***S*-63**.

Cpd.	Administration Route and Dosage	C_{max} (ng/mL)[a]	$T_{1/2}$ (h)[a]	AUC_{0-t} (h ng/mL)[a]	Vss (L/kg)[a]	CL (mL/kg/min)[a]	F%[a]
***S*-63**	iv (2 mg/kg)	_	0.518±0.121	1400±446	0.853±0.0854	25.8±9.67	29.2±14.7
	po (10 mg/kg)	643±413	1.20±0.256	2009±993	_	_	
Idelalisib	iv (2 mg/kg)	_	0.519 ± 0.091	1396 ± 298	0.884±0.044	24.5±4.83	45.8±11.5
	po (10 mg/kg)	2317±1075	1.03±0.0541	3191±802	_	_	

a. Data were shown as mean ± SD (n=3).

2.6. Molecular Docking

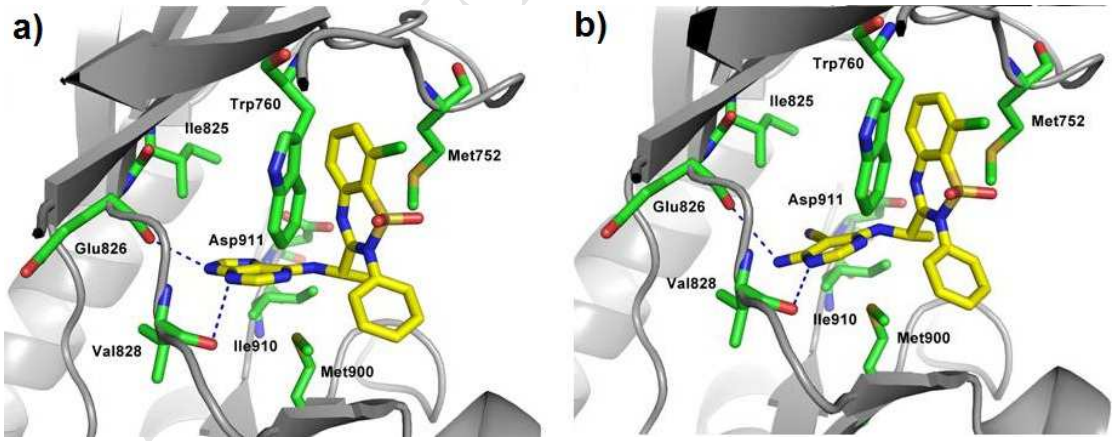

Figure 4. The molecular docking of ***S*-63** (a) and ***S*-71** (b) into the PI3Kδ active site.

The molecular docking analysis of ***S*-63** and ***S*-71** was carried out to elucidate their possible binding modes with PI3Kδ active site (**Figure 4**). Consequently, the purine moiety of ***S*-63** was engaged in H-bond contacts with residues Glu826 and Val828 in the hinge region, while the benzothiadiazine

template inserted deeply into the allosteric specificity pocket with Trp760 on one side and Met752 on the other side (**Figure 4a**). Similarly, ***S*-71** formed two H-bonds with residues in the hinge region, while the benzothiadiazine core occupied the allosteric selectivity pocket (**Figure 4b**). These results of molecular simulation may account for the PI3Kδ inhibitory potency and the subtype selectivity of ***S*-63** and ***S*-71**.

3. Conclusions

In summary, we have designed and synthesized a series of benzothiadiazine-based PI3Kδ-selective inhibitors *via* bioisosterism. Among these compounds, **63** and **71** displayed remarkable PI3Kδ inhibitory activity (IC_{50}s: below 10 nM), along with promising anti-proliferative potency against the B-cell leukemia SU-DHL-6 cells (GI_{50}s: below 1 μM). We next performed the chiral resolution of the key amine intermediate towards their synthesis and prepared corresponding enantiomers. In subsequent biological evaluation, ***S*-63** and ***S*-71** demonstrated comparable and superior PI3Kδ inhibitory activity, respectively, to that of idelalisib. Additionally, both compounds exerted enhanced anti-proliferative potency against the SU-DHL-6 cells compared to that of idelalisib. In terms of PI3Kδ selectivity, ***S*-63** and ***S*-71** were comparable and superior to idelalisib, respectively. Furthermore, the *S*-configuration was more beneficial to both PI3Kδ inhibitory activity and specificity than *R*-configuration. In further *in vivo* PK study, ***S*-63** displayed a good plasma exposure and an acceptable oral bioavailability of 29.2%. Owing to its favorable biological performance, ***S*-63** merits further development as a potential therapeutic agent for treating B-cell-mediated malignancies.

4. Experimental section

4.1. Chemistry

All the reagents and solvents were purchased from common commercial suppliers. If necessary, purification was carried out prior to use. Melting points were uncorrected and determined on a Büchi B-540 apparatus. ^{1}H and ^{13}CNMR spectra were recorded on a Bruker Avance III 500 (500 MHz) or Bruker Avance 400 II (400MHz) spectrometer in the indicated solvent. ESI-MS were obtained by Bruker Esquire-LC-00075 spectrometer, and HRMS were recorded on an Agilent 6224 TOF LC/MS spectrometer. Flash column chromatography was performed using silica gel (200–300 mesh). HPLC was performed using an Agilent 1200 system with UV detection at 254 nm, eluting with a binary solvent system A and B [A: MeOH; B: H_2O with 0.12% ammonium acetate (W/V)]. Analytical purity

of all target compounds was shown in the supplementary material. Chiral HPLC was performed on a Shimadzu LC-2010C system with UV detection at 254 nm, eluting with a binary solvent system C and D (C: i-PrOH; D: hexane).

*4.1.1. General procedure for intermediates **9** and **10***

2-Fluoro-6-nitrobenzenesulfonyl chloride **9** and 2-chloro-6-nitrobenzenesulfonyl chloride **10** were prepared according to a reported procedure from 1, 2-difluoro-3-nitrobenzene **7** and 1, 2-dichloro-3-nitrobenzene **8**, respectively, as light yellow solids.

*4.1.2. General procedure for intermediates **12-19***

To a solution of aniline (23 mL, 249 mmol, 1.1 eq) and pyridine (22 mL, 271 mmol, 1.2 eq) in anhydrous DCM (200 mL) was added a solution of 2-nitrobenzenesulfonyl chloride (50.0 g, 226 mmol, 1.0 eq) in anhydrous DCM (200 mL) dropwise at 0 ºC. The resultant mixture was stirred at room temperature for 0.5 h and then quenched with dilute hydrochloric acid (1 N). After filtration, the filtrate was washed with brine, dried over anhydrous Na_2SO_4, and concentrated in vacuo. The residue was ultimately subjected to recrystallization with EtOH to provide *N*-phenyl-2-nitrobenzenesulfonamide **12** as a light yellow solid. Yield 83%; ESI-MS: m/z = 279 $[M+H]^+$. Intermediates **13−19** were prepared in a procedure similar to that described for **12**.

N-(4-fluorophenyl)-2-nitrobenzenesulfonamide (**13**) Light yellow solid; yield 76%; ESI-MS: m/z = 297 $[M+H]^+$.

N-(3-(trifluoromethyl)phenyl)-2-nitrobenzenesulfonamide (**14**) Light yellow solid; yield 73%; ESI-MS: m/z = 347 $[M+H]^+$.

N-(4-(trifluoromethoxy)phenyl)-2-nitrobenzenesulfonamide (**15**) Light yellow solid; yield 82%; ESI-MS: m/z = 363 $[M+H]^+$.

N-(3,4-dimethoxyphenyl)-2-nitrobenzenesulfonamide (**16**) Light yellow solid; yield 89%; ESI-MS: m/z = 339 $[M+H]^+$.

N-(pyridin-3-yl)-2-nitrobenzenesulfonamide (**17**) The crude product was purified by flash column chromatography using EA/petroleum ether (PE) (1:2) as the eluent. Light yellow solid; yield 70%; ESI-MS: m/z = 280 $[M+H]^+$.

N-phenyl-2-fluoro-6-nitrobenzenesulfonamide (**18**) The crude product was purified by flash column chromatography using EA/PE (1:12–2:9) as the eluent. Light yellow solid; yield 68%; ^{1}H NMR (500 MHz, DMSO-d_6): δ 11.14 (s, 1H), 7.93–7.85 (m, 1H), 7.78 (d, 8.0 Hz, 1H), 7.73 (t, 9.0 Hz, 1H), 7.29 (t,

8.0 Hz, 2H), 7.16–7.02 (m, 3H); ESI-MS: m/z = 297 $[M+H]^+$.

N-phenyl-2-chloro-6-nitro-benzenesulfonamide (**19**) The crude product was purified by flash column chromatography using EA/PE (1:12–2:9) as the eluent. Light yellow solid; Yield 63%; ^{1}H NMR (500 MHz, DMSO-d_6): δ 11.14 (s, 1H), 7.91–7.85 (m, 2H), 7.81 (t, 8.0 Hz, 1H), 7.29–7.24 (m, 2H), 7.10–7.06 (m, 3H); ESI-MS: m/z = 313 $[M+H]^+$.

*4.1.3. General procedure for intermediates **20-31***

To a solution of **12** (25.0 g, 89.9 mmol, 1.0 eq) and $NiCl_2 \cdot 6H_2O$ (42.8 g, 180 mmol, 2.0 eq) in DCM (300 mL) and MeOH (100 mL) was added $NaBH_4$ (13.7 g, 360 mmol, 4.0 eq) carefully at 0 ºC. The resultant mixture was stirred at room temperature for 0.5 h and the solvent was removed under reduced pressure. The residue was then extracted with EA before filtration, and the filtrate was washed successively with H_2O and brine. After being dried over anhydrous Na_2SO_4, the organic layer was concentrated in vacuo to afford a clear and viscous oil that was slowly solidified. Yield 91%.

A solution of the newly afforded product (10.0 g, 40.3 mmol, 1.0 eq) in triethylorthopropionate (16 mL, 80.6 mmol, 2.0 eq) was stirred at 130 ºC under N_2 atmosphere. After TLC indicated the total conversion, removal of EtOH formed during the reaction and the excessive triethylorthopropionate under reduced pressure gave a viscous oil. Ph_2O (30 mL) was then added and the resultant solution boiled at 250 ºC under N_2 atmosphere for 4 h. Subsequently, it was totally cooled and kept at −10 ºC overnight. PE was added to the mixture, which was then stirred at room temperature. Following filtration, the precipitate was washed successively with PE and MeOH to afford 3-ethyl-2-phenyl-2*H*-benzo[*e*][1,2,4]thiadiazine 1,1-dioxide **20** as a pale solid. Yield 94% (for two steps); ^{1}H NMR (500 MHz, DMSO-d_6): δ 7.95 (dd, 1.5 Hz, 8.0 Hz, 1H), 7.88–7.82 (m, 1H), 7.67–7.63 (m, 1H), 7.62–7.56 (m, 4H), 7.53–7.48 (m, 2H), 2.33 (q, 7.5 Hz, 2H), 1.11 (t, 7.5 Hz, 3H); ESI-MS: m/z = 287 $[M+H]^+$. Intermediates **21**−**31** were prepared in a procedure similar to that described for **20**. For **21**−**29**, the reaction mixture of the intramolecular cyclization was directly subjected to flash column chromatography utilizing EA/PE (1:7) as the eluent to afford the product. As for **30** and **31**, the intramolecular cyclization occurred when the reduced product of **19** was treated with corresponding orthoester. After removal of EtOH and the excessive orthoester, the residue was purified by flash column chromatography utilizing EA/PE (1:7) as the eluent to afford the product.

3-Ethyl-2-(4-fluorophenyl)-2*H*-benzo[*e*][1,2,4]thiadiazine 1,1-dioxide (**21**) White solid; yield 84% (for three steps); ^{1}H NMR (500 MHz, DMSO-d_6): δ 7.96 (d, 8.0 Hz, 1H), 7.88–7.82 (m, 1H), 7.65 (d,

8.0 Hz, 1H), 7.63–7.56 (m, 3H), 7.43 (t, 8.5 Hz, 2H), 2.33 (q, 7.0 Hz, 2H), 1.11 (t, 7.0 Hz, 3H); ESI-MS: m/z = 305 $[M+H]^+$.

2-(4-Fluorophenyl)-3-propyl-2*H*-benzo[*e*][1,2,4]thiadiazine 1,1-dioxide (**22**) White solid; yield 80% (for three steps); ESI-MS: m/z = 319 $[M+H]^+$.

3-Ethyl-2-(3-(trifluoromethyl)phenyl)-2*H*-benzo[*e*][1,2,4]thiadiazine 1,1-dioxide (**23**) White solid; yield 79% (for three steps); ^{1}H NMR (500 MHz, DMSO-d_6): δ 8.00–7.95 (m, 3H), 7.91–7.81 (m, 3H), 7.66 (d, 9.5 Hz, 1H), 7.60 (t, 9.5 Hz, 1H), 2.33 (q, 9.0 Hz, 2H), 1.11 (t, 9.0 Hz, 3H); ESI-MS: m/z = 355 $[M+H]^+$.

3-Propyl-2-(3-(trifluoromethyl)phenyl)-2*H*-benzo[*e*][1,2,4]thiadiazine 1,1-dioxide (**24**) White solid; yield 73% (for three steps); ^{1}H NMR (500 MHz, DMSO-d_6): δ 8.00–7.92 (m, 3H), 7.89–7.81 (m, 3H), 7.66 (d, 9.5 Hz, 1H), 7.60 (t, 9.5 Hz, 1H), 2.30 (t, 9.0 Hz, 2H), 1.71–1.55 (m, 2H), 0.83 (t, 9.0 Hz, 3H); ESI-MS: m/z = 369 $[M+H]^+$.

3-Propyl-2-(4-(trifluoromethoxy)phenyl)-2*H*-benzo[*e*][1,2,4]thiadiazine 1,1-dioxide (**25**) White solid; yield 84% (for three steps); ^{1}H NMR (500 MHz, DMSO-d_6): δ 7.96 (d, 7.5 Hz, 1H), 7.86 (t, 8.0 Hz, 1H), 7.71–7.64 (m, 3H), 7.62–7.55 (m, 3H), 2.32 (t, 7.5 Hz, 2H), 1.67–1.59 (m, 2H), 0.85 (t, 7.5 Hz, 3H); ESI-MS: m/z = 385 $[M+H]^+$.

2-(3,4-Dimethoxyphenyl)-3-propyl-2*H*-benzo[*e*][1,2,4]thiadiazine 1,1-dioxide (**26**) White solid; yield 78% (for three steps); ^{1}H NMR (500 MHz, DMSO-d_6): δ 7.94 (dd, 1.5 Hz, 7.5 Hz, 1H), 7.86–7.79 (m, 1H), 7.62 (d, 8.0 Hz, 1H), 7.59–7.56 (m, 1H), 7.12 (d, 8.5 Hz, 1H), 7.06 (dd, 2.5 Hz, 8.5 Hz, 1H), 7.01 (d, 2.5 Hz, 1H), 3.84 (s, 3H), 3.76 (s, 3H), 2.34 (t, 7.5 Hz, 2H), 1.70–1.61 (m, 2H), 0.86 (t, 7.5 Hz, 3H); ESI-MS: m/z = 361 $[M+H]^+$.

3-Ethyl-2-(pyridin-3-yl)-2*H*-benzo[*e*][1,2,4]thiadiazine 1,1-dioxide (**27**) White solid; yield 62% (for three steps); ^{1}H NMR (500 MHz, DMSO-d_6): δ 8.78 (dd, 1.5 Hz, 5.0 Hz, 1H), 8.72 (d, 2.5 Hz, 1H), 8.07–8.03 (m, 1H), 7.98 (dd, 1.0 Hz, 8.0 Hz, 1H), 7.89–7.85 (m, 1H), 7.69–7.60 (m, 3H), 2.34 (q, 7.5 Hz, 2H), 1.12 (t, 7.5 Hz, 3H); ESI-MS: m/z = 288 $[M+H]^+$.

3-Ethyl-8-fluoro-2-phenyl-2*H*-benzo[*e*][1,2,4]thiadiazine 1,1-dioxide (**28**) White solid; yield 78% (for two steps); ^{1}H NMR (500 MHz, DMSO-d_6): δ 7.90–7.83 (m, 1H), 7.63–7.58 (m, 3H), 7.57–7.52 (m, 2H), 7.51–7.43 (m, 2H), 2.30 (q, 7.5 Hz, 2H), 1.10 (t, 7.5 Hz, 3H); ESI-MS: m/z = 305 $[M+H]^+$.

8-Fluoro-2-phenyl-3-propyl-2*H*-benzo[*e*][1,2,4]thiadiazine 1,1-dioxide (**29**) White solid; yield 81% (for two steps); ^{1}H NMR (500 MHz, DMSO-d_6): δ 7.89–7.81 (m, 1H), 7.63–7.58 (m, 3H), 7.55–7.51

(m, 2H), 7.50–7.44 (m, 2H), 2.28 (t, 7.0 Hz, 2H), 1.65–1.57 (m, 2H), 0.82 (t, 7.5 Hz, 3H); ESI-MS: m/z = 319 $[M+H]^+$.

8-Chloro-3-ethyl-2-phenyl-2*H*-benzo[*e*][1,2,4]thiadiazine 1,1-dioxide (**30**) White solid; yield 78% (for two steps); ^{1}H NMR (500 MHz, DMSO-d_6): δ 7.84–7.76 (m, 1H), 7.70–7.50 (m, 7H), 2.28 (q, 9.0 Hz, 2H), 1.09 (t, 9.0 Hz, 3H); ESI-MS: m/z = 321 $[M+H]^+$.

8-Chloro-2-phenyl-3-propyl-2*H*-benzo[*e*][1,2,4]thiadiazine 1,1-dioxide (**31**) White solid; yield 80% (for two steps); ^{1}H NMR (500 MHz, DMSO-d_6): δ 7.80 (t, 8.5 Hz, 1H), 7.66 (dd, 1.0 Hz, 8.0 Hz, 1H), 7.63–7.57 (m, 4H), 7.55–7.50 (m, 2H), 2.67 (t, 7.5 Hz, 2H), 1.65–1.57 (m, 2H), 0.82 (t, 7.5 Hz, 3H); ESI-MS: m/z = 335 $[M+H]^+$.

*4.1.4. General procedure for intermediates **32-43***

To a solution of **20** (6.00 g, 20.9 mmol, 1.0 eq) and AcONa (2.41 g, 29.3 mmol, 1.4 eq) in AcOH (40 mL) were carefully added Br_2 (1.50 mL, 29.3 mmol, 1.4 eq), and the resultant mixture was stirred at 40 ºC till TLC demonstrated total conversion of **20**. After the reaction mixture was cooled, water was added to quench the reaction and the deposit collected by filtration. The solution of the filter cake in DCM was then washed with saturated $Na_2S_2O_3$ solution, brine, dried over Na_2SO_4, and concentrated in vacuo. The residue was subjected to recrystallization using EA to afford 3-(1-bromoethyl)-2-phenyl-2*H*-benzo[*e*][1,2,4]thiadiazine 1,1-dioxide **32** as a white solid. Yield 91%; ^{1}H NMR (500 MHz, DMSO-d_6): δ 7.99 (dd, 1.5 Hz, 8.0 Hz, 1H), 7.94–7.88 (m, 1H), 7.75 (dd, 1.0 Hz, 8.0 Hz, 1H), 7.68 (dt, 1.0 Hz, 8.0 Hz, 1H), 7.65–7.42 (m, 5H), 4.55 (q, 6.5 Hz, 1H), 1.93 (t, 6.5 Hz, 3H); ESI-MS: m/z = 365 $[M+H]^+$. Intermediates **33−43** were prepared in a procedure similar to that described for **32**. The crude product was purified by flash column chromatography utilizing EA/PE (1:10) as the eluent.

3-(1-Bromoethyl)-2-(4-fluorophenyl)-2*H*-benzo[*e*][1,2,4]thiadiazine 1,1-dioxide (**33**) White solid; yield 83%; ^{1}H NMR (500 MHz, DMSO-d_6): δ 7.99 (dd, 1.0 Hz, 8.0 Hz, 1H), 7.95–7.87 (m, 1H), 7.75 (d, 8.0 Hz, 1H), 7.72–7.54 (m, 3H), 7.45 (t, 8.0 Hz, 2H), 4.59 (q, 6.5 Hz, 1H), 1.93 (t, 6.5 Hz, 3H); ESI-MS: m/z = 383 $[M+H]^+$.

3-(1-Bromopropyl)-2-(4-fluorophenyl)-2*H*-benzo[*e*][1,2,4]thiadiazine 1,1-dioxide (**34**) White solid; yield 85%; ^{1}H NMR (500 MHz, DMSO-d_6): δ 8.00 (dd, 1.0 Hz, 7.5 Hz, 1H), 7.95–7.87 (m, 1H), 7.73 (d, 7.5 Hz, 1H), 7.70–7.67 (m, 1H), 7.61 (s, 2H), 7.46 (t, 7.5 Hz, 2H), 4.30 (q, 7.0 Hz, 1H), 2.42–2.33 (m, 1H), 2.18–2.09 (m, 1H), 0.94 (t, 7.0 Hz, 3H); ESI-MS: m/z = 397 $[M+H]^+$.

3-(1-Bromoethyl)-2-(3-(trifluoromethyl)phenyl)-2*H*-benzo[*e*][1,2,4]thiadiazine 1,1-dioxide (**35**) White solid; yield 79%; ^{1}H NMR (500 MHz, DMSO-d_6): δ 8.02–7.97 (m, 3H), 7.92 (t, 9.5 Hz, 2H), 7.85 (t, 9.5 Hz, 1H), 7.76 (d, 10.5 Hz, 1H), 7.69 (d, 9.5 Hz, 1H), 4.58 (q, 8.0 Hz, 1H), 1.94 (d, 8.0 Hz, 3H); ESI-MS: m/z = 433 $[M+H]^+$.

3-(1-Bromopropyl)-2-(3-(trifluoromethyl)phenyl)-2*H*-benzo[*e*][1,2,4]thiadiazine 1,1-dioxide (**36**) White solid; yield 79%; ^{1}H NMR (500 MHz, DMSO-d_6): δ 8.03–7.99 (m, 2H), 7.96–7.82 (m, 4H), 7.75 (d, 10.5 Hz, 1H), 7.69 (t, 9.5 Hz, 1H), 4.29 (t, 9.0 Hz, 1H), 2.44–2.31 (m, 1H), 2.18–2.07 (m, 1H), 0.94 (t, 9.0 Hz, 3H); ESI-MS: m/z = 447 $[M+H]^+$.

3-(1-Bromopropyl)-2-(4-(trifluoromethoxy)phenyl)-2*H*-benzo[*e*][1,2,4]thiadiazine 1,1-dioxide (**37**) White solid; yield 84%; ^{1}H NMR (500 MHz, DMSO-d_6): δ 8.00 (d, 9.5 Hz, 1H), 7.91 (t, 9.5 Hz, 1H), 7.83–7.52 (m, 6H), 4.32 (t, 9.0 Hz, 1H), 2.43–2.31 (m, 1H), 2.21–2.07 (m, 1H), 0.94 (t, 9.0 Hz, 3H); ESI-MS: m/z = 463 $[M+H]^+$.

3-(1-Bromopropyl)-2-(3,4-dimethoxyphenyl)-2*H*-benzo[*e*][1,2,4]thiadiazine 1,1-dioxide (**38**) White solid; yield 93%; ^{1}H NMR (500 MHz, DMSO-d_6): δ 7.99 (dd, 1.5 Hz, 7.5 Hz, 1H), 7.92–7.86 (m, 1H), 7.71 (dd, 1.0 Hz, 8.5 Hz, 1H), 7.68–7.65 (m, 1H), 7.31–6.88 (m, 3H), 4.33 (t, 7.5 Hz, 1H), 3.84 (s, 3H), 3.74 (s, 3H), 2.43–2.33 (m, 1H), 2.14–2.08 (m, 1H), 0.93 (t, 7.0 Hz, 3H); ESI-MS: m/z = 439 $[M+H]^+$.

3-(1-Bromoethyl)-2-(pyridin-3-yl)-2*H*-benzo[*e*][1,2,4]thiadiazine 1,1-dioxide (**39**) White solid; yield 76%; ESI-MS: m/z = 366 $[M+H]^+$.

3-(1-Bromoethyl)-8-fluoro-2-phenyl-2*H*-benzo[*e*][1,2,4]thiadiazine 1,1-dioxide (**40**) White solid; yield 89%; ^{1}H NMR (500 MHz, DMSO-d_6): δ 7.97–7.87 (m, 1H), 7.71–7.45 (m, 7H), 4.51 (q, 6.5 Hz, 1H), 1.91 (d, 6.5 Hz, 3H); ESI-MS: m/z = 383 $[M+H]^+$.

3-(1-Bromopropyl)-8-fluoro-2-phenyl-2*H*-benzo[*e*][1,2,4]thiadiazine 1,1-dioxide (**41**) White solid; yield 86%; ESI-MS: m/z = 397 $[M+H]^+$.

3-(1-Bromoethyl)-8-chloro-2-phenyl-2*H*-benzo[*e*][1,2,4]thiadiazine 1,1-dioxide (**42**) White solid; yield 92%; ^{1}H NMR (500 MHz, DMSO-d_6): δ 7.62–7.57 (m, 3H), 7.56–7.50 (m, 4H), 7.48 (dd, 2.0 Hz, 7.0 Hz, 1H), 4.38 (q, 7.0 Hz, 1H), 1.96 (d, 6.5 Hz, 3H); ESI-MS: m/z = 399 $[M+H]^+$.

3-(1-Bromopropyl)-8-chloro-2-phenyl-2*H*-benzo[*e*][1,2,4]thiadiazine 1,1-dioxide (**43**) White solid; yield 87%; ^{1}H NMR (500 MHz, DMSO-d_6): δ 7.86 (t, 8.5 Hz, 1H), 7.75 (dd, 1.0 Hz, 8.0 Hz, 1H), 7.68 (dd, 1.0 Hz, 8.0 Hz, 1H), 7.65–7.42 (m, 5H), 4.19 (t, 7.5 Hz, 1H), 2.40–2.31 (m, 1H), 2.15–2.06 (m, 1H), 0.92 (d, 7.0 Hz, 3H); ESI-MS: m/z = 413 $[M+H]^+$.

*4.1.5. General procedure for intermediates **44-54***

To a solution of **32** (7.86 g, 21.6 mmol, 1.0 eq) and phthalimide (3.18 g, 21.6 mmol, 1.0 eq) in anhydrous DMF (30 mL) was added anhydrous K_2CO_3 (4.47 g, 32.4 mmol, 1.5 eq). The resultant mixture was stirred at 40 ºC for 6 h, and H_2O was added under agitation to quench the reaction. After filtration, the solution of the filter cake in DCM was washed successively with H_2O and brine, dried over anhydrous Na_2SO_4, and concentrated in vacuo. To the residue, EtOH (100 mL) and hydrazine hydrate (85%, 2.6 mL, 43.2 mmol, 2.0 eq) were added. The resultant mixture was stirred at 80 ºC under N_2 atmosphere till TLC demonstrated total conversion of the substrate. After the reaction mixture was completely cooled, the precipitate was filtered and the filtrate was concentered in vacuo. To the residue EA was added, and the undissolved component was filtered. The filtrate was subsequently washed successively with NaOH solution (0.5 N) and brine, dried over anhydrous Na_2SO_4, and concentrated in vacuo. Final flash column chromatography utilizing EA/PE/TEA (60:60:1) as the eluent afforded 3-(1-aminoethyl)-2-phenyl-2*H*-benzo[*e*][1,2,4]thiadiazine 1,1-dioxide **44** as a light yellow oil that was slowly solidified. Yield 52% (for two steps); ESI-MS: m/z = 302 $[M+H]^+$. Intermediates **45−54** were prepared in a procedure similar to that described for **44**.

3-(1-Aminoethyl)-2-(4-fluorophenyl)-2*H*-benzo[*e*][1,2,4]thiadiazine 1,1-dioxide (**45**) Light yellow oil; yield 39% (for two steps); ESI-MS: m/z = 320 $[M+H]^+$.

3-(1-Aminoethyl)-2-(3-(trifluoromethyl)phenyl)-2*H*-benzo[*e*][1,2,4]thiadiazine 1,1-dioxide (**46**) Light yellow oil; yield 32% (for two steps); ESI-MS: m/z = 370 $[M+H]^+$.

3-(1-Aminopropyl)-2-(3-(trifluoromethyl)phenyl)-2*H*-benzo[*e*][1,2,4]thiadiazine 1,1-dioxide (**47**) Light yellow oil; yield 54% (for two steps); ESI-MS: m/z = 384 $[M+H]^+$.

3-(1-Aminopropyl)-2-(4-(trifluoromethoxy)phenyl)-2*H*-benzo[*e*][1,2,4]thiadiazine 1,1-dioxide (**48**) Light yellow oil; yield 50% (for two steps); ESI-MS: m/z = 400 $[M+H]^+$.

3-(1-Aminopropyl)-2-(3,4-dimethoxyphenyl)-2*H*-benzo[*e*][1,2,4]thiadiazine 1,1-dioxide (**49**) Light yellow oil; yield 55% (for two steps); ESI-MS: m/z = 376 $[M+H]^+$.

3-(1-Aminoethyl)-2-(pyridin-3-yl)-2*H*-benzo[*e*][1,2,4]thiadiazine 1,1-dioxide (**50**) Light yellow oil; yield 34% (for two steps); ESI-MS: m/z = 303 $[M+H]^+$.

3-(1-Aminoethyl)-8-fluoro-2-phenyl-2*H*-benzo[*e*][1,2,4]thiadiazine 1,1-dioxide (**51**) Light yellow oil; yield 37% (for two steps); ESI-MS: m/z = 320 $[M+H]^+$.

3-(1-Aminopropyl)-8-fluoro-2-phenyl-2*H*-benzo[*e*][1,2,4]thiadiazine 1,1-dioxide (**52**) Light yellow

solid; yield 53% (for two steps); ^{1}H NMR (500 MHz, DMSO-d_6): δ 7.91–7.82 (m, 1H), 7.66–7.56 (m, 3H), 7.55–7.45 (m, 4H), 3.14–3.07 (m, 1H), 2.03 (brs, 2H), 1.74–1.63 (m, 1H), 1.47–1.37 (m, 1H), 0.76 (t, 7.5 Hz, 3H); ESI-MS: m/z = 334 $[M+H]^+$.

3-(1-Aminoethyl)-8-chloro-2-phenyl-2*H*-benzo[*e*][1,2,4]thiadiazine 1,1-dioxide (**53**) Light yellow oil; yield 40% (for two steps); ESI-MS: m/z = 336 $[M+H]^+$.

3-(1-Aminopropyl)-8-chloro-2-phenyl-2*H*-benzo[*e*][1,2,4]thiadiazine 1,1-dioxide (**54**) Light yellow solid; yield 56% (for two steps); ^{1}H NMR (500 MHz, DMSO-d_6): δ 7.81 (t, 8.0 Hz, 1H), 7.67 (dd, 1.0 Hz, 8.0 Hz, 1H), 7.64 (dd, 1.0 Hz, 8.5 Hz, 1H), 7.61–7.56 (m, 3H), 7.55–7.46 (m, 2H), 3.14–3.02 (m, 1H), 2.00 (brs, 2H), 1.76–1.61 (m, 1H), 1.47–1.35 (m, 1H), 0.77 (t, 7.5 Hz, 3H); ESI-MS: m/z = 350 $[M+H]^+$.

*4.1.6. General procedure for target compounds **55-72***

To the solution of **44** (200 mg, 0.664 mmol, 1.1 eq) in *t*-BuOH (4 mL) were added 6-chloro-9*H*-purine (93 mg, 0.604 mmol, 1.0 eq) and DIPEA (149 μL, 0.906 mmol, 1.5 eq). The resultant mixture was stirred at 80 ºC under N_2 atmosphere for 8 h and concentrated in vacuo. To the residue was added DCM, and the mixture was washed successively with saturated $NaHCO_3$ solution, dilute hydrochloric acid (0.5 N) and brine. The organic layer was dried over anhydrous Na_2SO_4 and concentrated in vacuo. Flash column chromatography utilizing EA/PE (1:1–3:1) and EA/AcOH (80:1) as the eluent afforded a light yellow oil. It was then dissolved in DCM, and the resulting solution was washed successively with saturated $NaHCO_3$ solution, brine, dried over anhydrous Na_2SO_4, and concentrated in vacuo to afford 3-(1-((9*H*-purin-6-yl)amino)ethyl)-2-phenyl-2*H*-benzo[*e*][1,2,4]thiadiazine 1,1-dioxide **55** as a light yellow solid. Yield 28%; ^{1}H NMR (500 MHz, DMSO-d_6): δ 12.96 (s, 0.7H), 12.10 (s, 0.3H), 8.31–8.09 (m, 2H), 7.94 (d, 7.5 Hz, 2H), 7.80 (t, 7.5 Hz, 1H), 7.68–7.50 (m, 7H), 4.91–4.71 (m, 1H), 1.48 (d, 7.0 Hz, 3H); ^{13}C NMR (125 MHz, DMSO-d_6): δ 158.79, 153.40, 152.38, 142.09, 139.70, 134.82, 132.52, 130.65, 130.46, 130.11, 129.86, 129.73, 128.24, 128.19, 127.09, 121.95, 48.54, 18.83; ESI-HRMS: m/z calcd for $C_{20}H_{17}N_7O_2S$ $[M+H]^+$ 420.1243, found 420.1235; HPLC: t_R = 15.19 min, flow rate 1.2 mL/min, Diamonsil^{TM} C18 5μ 4.6×200 mm, rt, eluent A-75%, eluent B-25%.

Compound **56-72** were prepared in a manner similar to that described for **55**. As for compounds **68-72**, the products were precipitated from the reaction mixture and obtained by filtration without further treatment.

3-(1-((9*H*-purin-6-yl)amino)ethyl)-2-(4-fluorophenyl)-2*H*-benzo[*e*][1,2,4]thiadiazine 1,1-dioxide (**56**) Light yellow solid; yield 21%; ^{1}H NMR (500 MHz, $CDCl_3$): δ 8.36 (s, 1H), 8.05 (s, 1H), 7.90 (dd, 1.5 Hz, 8.0 Hz, 1H), 7.71 (t, 7.5 Hz, 1H), 7.64 (d, 7.5 Hz, 1H), 7.60–7.46 (m, 3H), 7.28–7.18 (m, 2H), 7.12–7.03 (m, 1H), 5.21–4.94 (m, 1H), 1.61 (d, 7.0 Hz, 3H); ^{13}C NMR (125 MHz, DMSO-d_6): δ 163.22 (d, J_{C-F} = 247.5 Hz), 158.64, 152.29, 144.01, 142.06, 134.88, 132.93, 128.25 (d, J_{C-F} = 8.75 Hz), 126.93, 122.71 (d, J_{C-F} = 8.75 Hz), 122.01, 121.74, 118.87, 117.00 (d, J_{C-F} = 22.5 Hz), 116.61 (d, J_{C-F} = 22.5 Hz), 114.47, 48.47, 18.77; ESI-HRMS: m/z calcd for $C_{20}H_{16}FN_7O_2S$ $[M+H]^+$ 438.1148, found 438.1146; HPLC: t_R = 7.67 min, flow rate 1.0 mL/min, COSMOSIL 5C18-MS-II column (4.6ID×250 mm), rt, eluent A-65%, eluent B-35%.

3-(1-((9*H*-purin-6-yl)amino)ethyl)-2-(3-(trifluoromethyl)phenyl)-2*H*-benzo[*e*][1,2,4]thiadiazine 1,1-dioxide (**57**) Light yellow solid; yield 25%; ^{1}H NMR (500 MHz, DMSO-d_6): δ 12.95 (s, 1H), 8.17 (s, 2H), 8.07–7.88 (m, 4H), 7.84 (t, 7.0 Hz, 2H), 7.77–7.67 (m, 1H), 7.66–7.55 (m, 2H), 4.93–4.81 (m, 1H), 1.50 (d, 7.0 Hz, 3H); ESI-HRMS: m/z calcd for $C_{21}H_{16}F_3N_7O_2S$ $[M+H]^+$ 488.1117, found 488.1122; HPLC: t_R = 7.87 min, flow rate 1.0 mL/min, COSMOSIL 5C18-MS-II column (4.6ID×250 mm), rt, eluent A-70%, eluent B-30%.

3-(1-((9*H*-purin-6-yl)amino)propyl)-2-(3-(trifluoromethyl)phenyl)-2*H*-benzo[*e*][1,2,4]thiadiazine 1,1-dioxide (**58**) Light yellow solid; yield 40%; ^{1}H NMR (500 MHz, DMSO-d_6): δ 12.96 (s, 1H), 8.18 (s, 1H), 8.11–7.70 (m, 8H), 7.68-7.54 (m, 2H), 4.82–4.55 (m, 1H), 2.11–1.85 (m, 2H), 0.86 (t, 6.5 Hz, 3H); ^{13}C NMR (125 MHz, DMSO-d_6): δ 157.14, 154.33, 153.81, 151.91, 149.29, 141.95, 140.46, 139.86, 139.15, 134.99, 134.47, 133.37, 131.39, 130.63 (q, J_{C-F} = 32.5 Hz), 128.47, 127.27, 127.09, 123.82 (q, J_{C-F} = 270 Hz), 121.94, 53.96, 25.95, 11.09; ESI-HRMS: m/z calcd for $C_{22}H_{18}F_3N_7O_2S$ $[M+H]^+$ 502.1273, found 502.1277; HPLC: t_R = 10.56 min, flow rate 1.0 mL/min, COSMOSIL 5C18-MS-II column (4.6ID×250 mm), rt, eluent A-70%, eluent B-30%.

3-(1-((9*H*-purin-6-yl)amino)propyl)-2-(4-(trifluoromethoxy)phenyl)-2*H*-benzo[*e*][1,2,4]thiadiazine 1,1-dioxide (**59**) Light yellow solid; yield 47%; ^{1}H NMR (500 MHz, DMSO-d_6): δ 12.98 (s, 0.85H), 12.12 (s, 0.15H), 8.30 (s, 0.3H), 8.22–8.04 (m, 1.7H), 7.95 (d, 7.0 Hz, 2H), 7.82 (t, 7.0 Hz, 1H), 7.78–7.66 (m, 2H), 7.65–7.44 (m, 4H), 4.85–4.56 (m, 1H), 2.08–1.80 (m, 2H), 0.86 (t, 7.0 Hz, 3H); ESI-HRMS: m/z calcd for $C_{22}H_{18}F_3N_7O_3S$ $[M+H]^+$ 518.1222, found 518.1214; HPLC: t_R = 13.16 min, flow rate 1.0 mL/min, COSMOSIL 5C18-MS-II column (4.6ID×250 mm), rt, eluent A-70%, eluent B-30%.

3-(1-((9*H*-purin-6-yl)amino)propyl)-2-(3,4-dimethoxyphenyl)-2*H*-benzo[*e*][1,2,4]thiadiazine 1,1-dioxide (**60**) Light yellow solid; yield 40%; ^{1}H NMR (500 MHz, $CDCl_3$): δ 8.30 (s, 1H), 8.03 (s, 1H), 7.89 (dd, 1.5 Hz, 7.5 Hz, 1H), 7.73–7.61 (m, 2H), 7.51–7.44 (m, 1H), 7.17–6.76 (m, 3H), 5.28–5.12 (m, 1H), 3.96 (s, 3H), 3.79 (s, 3H), 2.17–2.06 (m, 1H), 1.96–1.86 (m, 1H), 0.98 (t, 7.0 Hz, 3H); ^{13}C NMR (125 MHz, DMSO-d_6): δ 157.88, 153.76, 152.29, 150.55, 149.53, 146.74, 142.08, 139.65, 134.72, 128.32, 128.21, 128.10, 127.11, 124.56, 122.81, 121.97, 113.62, 112.04, 56.16, 56.07, 53.71, 26.22, 11.01; ESI-HRMS: m/z calcd for $C_{23}H_{23}N_7O_4S$ $[M+H]^+$ 494.1610, found 494.1607; HPLC: t_R = 9.68 min, flow rate 1.0 mL/min, COSMOSIL 5C18-MS-II column (4.6ID×250 mm), rt, eluent A-60%, eluent B-40%.

3-(1-((9*H*-purin-6-yl)amino)ethyl)-2-(pyridin-3-yl)-2*H*-benzo[*e*][1,2,4]thiadiazine 1,1-dioxide (**61**) Light yellow solid; yield 19%; ^{1}H NMR (500 MHz, DMSO-d_6): δ 12.96 (s, 0.8H), 12.01 (s, 0.2H), 8.77 (s, 1H), 8.66 (s, 1H), 8.29 (s, 0.2H), 8.18–8.10 (m, 1.8H), 8.08 (s, 2H), 7.97 (dd, 1.0 Hz, 8.0 Hz, 1H), 7.85–7.80 (m, 1H), 7.65–7.47 (m, 3H), 4.84–4.74 (m, 1H), 1.51 (d, 7.0 Hz, 3H); ESI-HRMS: m/z calcd for $C_{19}H_{16}N_8O_2S$ $[M+H]^+$ 421.1195, found 421.1197; HPLC: t_R = 6.91 min, flow rate 1.0 mL/min, COSMOSIL 5C18-MS-II column (4.6ID×250 mm), rt, eluent A-60%, eluent B-40%.

3-(1-((9*H*-purin-6-yl)amino)propyl)-8-fluoro-2-phenyl-2*H*-benzo[*e*][1,2,4]thiadiazine 1,1-dioxide (**62**) White solid; yield 46%; ^{1}H NMR (500 MHz, DMSO-d_6): δ 12.99 (s, 0.8H), 12.16 (s, 0.2H), 8.37–8.02 (m, 2H), 7.98–7.72 (m, 2H), 7.70–7.52 (m, 5H), 7.46 (t, 9.0 Hz, 1H), 7.36 (d, 7.5 Hz, 1H), 4.77–4.53 (m, 1H), 2.04–1.73 (m, 2H), 0.81 (t, 7.0 Hz, 3H); ^{13}C NMR (125 MHz, DMSO-d_6): δ 158.76, 156.29 (d, $J_{C\text{-}F}$ = 255 Hz), 153.96, 152.33, 150.40, 143.90, 139.70, 135.91 (d, $J_{C\text{-}F}$ = 10.00 Hz), 131.75, 130.92, 130.13, 124.59, 120.53, 119.33, 115.78 (d, $J_{C\text{-}F}$ = 12.50 Hz), 114.82 (d, $J_{C\text{-}F}$ = 20.00 Hz), 54.21, 25.91, 11.12; ESI-HRMS: m/z calcd for $C_{21}H_{18}FN_7O_2S$ $[M+H]^+$ 452.1305, found 452.1303; HPLC: t_R = 6.43 min, flow rate 1.0 mL/min, COSMOSIL 5C18-MS-II column (4.6ID×250 mm), rt, eluent A-70%, eluent B-30%.

3-(1-((9*H*-purin-6-yl)amino)ethyl)-8-chloro-2-phenyl-2*H*-benzo[*e*][1,2,4]thiadiazine 1,1-dioxide (**63**) Pale solid; yield 23%; ^{1}H NMR (500 MHz, DMSO-d_6): δ 12.97 (s, 0.8H), 12.06 (s, 0.2H), 8.29 (s, 0.2H), 8.20 (s, 0.2H), 8.17–8.10 (m, 1.6H), 8.02 (brs, 1H), 7.74 (t, 8.0 Hz, 1H), 7.70–7.61 (m, 3H), 7.60–7.50 (m, 3H), 7.48–7.43 (m, 1H), 4.79–4.65 (m, 1H), 1.47 (d, 7.0 Hz, 3H); ^{1}H NMR (500 MHz, $CDCl_3$): δ 8.33 (s, 1H), 7.97 (s, 1H), 7.63–7.47 (m, 7H), 7.42 (d, 6.0 Hz, 1H), 6.79 (brs, 1H), 5.28–4.91 (m, 1H), 1.56 (d, 5.0 Hz, 1H); ^{13}C NMR (125 MHz, DMSO-d_6): δ 159.21, 152.33, 144.26, 139.70,

135.07, 131.98, 131.04, 130.89, 130.14, 130.03, 129.66, 127.98, 127.94, 127.89, 125.22, 119.27, 48.54, 18.17; ESI-HRMS: m/z calcd for $C_{20}H_{16}ClN_7O_2S$ $[M+H]^+$ 454.0853, found 454.0851; HPLC: t_R = 7.74 min, flow rate 1.2 mL/min, COSMOSIL 5C18-MS-II column (4.6ID×250 mm), rt, eluent A-65%, eluent B-35%.

3-(1-((9*H*-purin-6-yl)amino)propyl)-8-chloro-2-phenyl-2*H*-benzo[*e*][1,2,4]thiadiazine 1,1-dioxide (**64**) White solid; yield 51%; ^{1}H NMR (500 MHz, $CDCl_3$): δ 13.87 (brs, 1H), 8.35 (s, 1H), 8.05 (s, 1H), 7.69–7.36 (m, 8H), 6.88 (d, 7.0 Hz, 1H), 5.20–4.97 (m, 1H), 2.14–2.07 (m, 1H), 1.95–1.86 (m, 1H), 0.98 (t, 7.0 Hz, 3H); ^{13}C NMR (125 MHz, DMSO-d_6): δ 158.31, 153.25, 152.24, 144.14, 140.53, 135.09, 132.07, 130.93, 130.08, 129.81, 129.77, 128.30, 127.99, 127.87, 125.35, 121.69, 54.14, 25.92, 11.07; ESI-MS: m/z = 468 $[M+H]^+$; HPLC: t_R = 10.75 min, flow rate 1.2 mL/min, COSMOSIL 5C18-MS-II column (4.6ID×250 mm), rt, eluent A-65%, eluent B-35%.

3-(1-((2-Fluoro-9*H*-purin-6-yl)amino)ethyl)-2-phenyl-2*H*-benzo[*e*][1,2,4]thiadiazine 1,1-dioxide (**65**) Pale solid; yield 46%; ^{1}H NMR (500 MHz, DMSO-d_6): δ 13.15–12.93 (m, 0.8H), 12.12 (s, 0.2H), 8.71 (d, 4.5 Hz, 0.7H), 8.43–8.23 (m, 0.6H), 8.14 (s, 0.7H), 7.95 (d, 7.0 Hz, 1H), 7.86–7.76 (m, 1H), 7.67–7.43 (m, 7H), 4.84–4.65 (m, 1H), 1.49 (d, 6.0 Hz, 3H); ^{13}C NMR (125 MHz, DMSO-d_6): δ 158.61 (d, J_{C-F} = 202.5 Hz), 157.87, 155.16, 151.55, 142.01, 134.88, 132.44, 132.38, 130.65, 130.30, 130.07, 129.72, 128.33, 128.30, 127.07, 121.99, 48.76, 18.53; ESI-HRMS: m/z calcd for $C_{20}H_{16}FN_7O_2S$ $[M+H]^+$ 438.1148, found 438.1146; HPLC: t_R = 7.28 min, flow rate 1.2 mL/min, COSMOSIL 5C18-MS-II column (4.6ID×250 mm), rt, eluent A-65%, eluent B-35%.

3-(1-((2-Chloro-9*H*-purin-6-yl)amino)ethyl)-2-phenyl-2*H*-benzo[*e*][1,2,4]thiadiazine 1,1-dioxide (**66**) Pale solid; yield 38%; ^{1}H NMR (500 MHz, DMSO-d_6): δ 13.14 (brs, 1H), 8.68 (s, 0.8H), 8.46–8.12 (m, 1.2H), 8.05–7.90 (m, 1H), 7.80 (t, 7.0 Hz, 1H), 7.74–7.64 (m, 2H), 7.63–7.28 (m, 5H), 4.83–4.61 (m, 1H), 1.48 (d, 6.0 Hz, 3H); ^{13}C NMR (125 MHz, DMSO-d_6): δ 158.06, 152.88, 142.01, 140.35, 135.15, 134.88, 133.07, 132.36, 130.69, 130.30, 130.14, 129.70, 128.29, 127.08, 125.00, 121.99, 48.67, 18.30; ESI-HRMS: m/z calcd for $C_{20}H_{16}ClN_7O_2S$ $[M+H]^+$ 454.0853, found 454.0854; HPLC: t_R = 7.77 min, flow rate 1.2 mL/min, COSMOSIL 5C18-MS-II column (4.6ID×250 mm), rt, eluent A-70%, eluent B-30%.

8-Fluoro-3-(1-((2-fluoro-9*H*-purin-6-yl)amino)propyl)-2-phenyl-2*H*-benzo[*e*][1,2,4]thiadiazine 1,1-dioxide (**67**) Pale solid; yield 42%; ^{1}H NMR (500 MHz, $CDCl_3$): δ 8.00 (s, 1H), 7.68–7.44 (m, 7H), 7.40 (d, 8.5 Hz, 1H), 7.17 (t, 8.5 Hz, 1H), 7.11 (d, 8.0 Hz, 1H), 4.99–4.87 (m, 1H), 2.15–2.02 (m, 1H),

1.97–1.84 (m, 1H), 0.97 (d, 7.0 Hz, 3H); ^{13}C NMR (125 MHz, DMSO-d_6): δ 158.58 (d, J_{C-F} = 204 Hz), 158.02, 157.33, 156.65 (d, J_{C-F} = 273 Hz), 155.73, 155.29, 144.58, 143.84, 140.15, 135.98 (d, J_{C-F} = 8.25 Hz), 131.59, 130.90 (d, J_{C-F} = 21.25 Hz), 130.26, 130.10, 124.66 (d, J_{C-F} = 2.50 Hz), 115.93 (d, J_{C-F} = 20.0 Hz), 54.67, 25.51, 11.35; ESI-HRMS: m/z calcd for $C_{21}H_{17}F_2N_7O_2S$ $[M+H]^+$ 470.1211, found 470.1227; HPLC: t_R = 7.86 min, flow rate 1.0 mL/min, COSMOSIL 5C18-MS-II column (4.6ID×250 mm), rt, eluent A-70%, eluent B-30%.

4-Amino-6-((1-(1,1-dioxido-2-phenyl-2*H*-benzo[*e*][1,2,4]thiadiazin-3-yl)ethyl)amino)pyrimidine-5-carbonitrile (**68**) Yield 63%; ^{1}H NMR (500 MHz, DMSO-d_6): δ 7.96 (dd, 1.5 Hz, 7.5 Hz, 1H), 7.93 (s, 1H), 7.87–7.81 (m, 1H), 7.69 (d, 7.0 Hz, 1H), 7.64–7.50 (m, 7H), 7.32 (brs, 2H), 4.73–4.65 (m, 1H), 1.40 (d, 7.0 Hz, 3H); ^{13}C NMR (125 MHz, DMSO-d_6): δ 170.03, 167.26, 165.12, 163.24, 147.28, 140.23, 137.73, 135.94, 135.65, 135.44, 133.62, 133.61, 132.40, 127.32, 121.05, 73.97, 54.32, 23.83; ESI-HRMS: m/z calcd for $C_{20}H_{17}N_7O_2S$ $[M+H]^+$ 420.1243, found 420.1241; HPLC: t_R = 7.38 min, flow rate 1.0 mL/min, COSMOSIL 5C18-MS-II column (4.6ID×250 mm), rt, eluent A-65%, eluent B-35%.

4-Amino-6-((1-(8-fluoro-1,1-dioxido-2-phenyl-2*H*-benzo[*e*][1,2,4]thiadiazin-3-yl)ethyl)amino)pyrimidine-5-carbonitrile (**69**) White solid, yield 58%; ^{1}H NMR (500 MHz, DMSO-d_6): δ 7.93 (s, 1H), 7.89–7.82 (m, 1H), 7.70 (d, 7.0 Hz, 1H), 7.63–7.58 (m, 2H), 7.57–7.53 (m, 3H), 7.51–7.47 (m, 1H), 7.43 (d, 8.0 Hz, 1H), 7.31 (brs, 2H), 4.72–4.58 (m, 1H), 1.40 (d, 7.0 Hz, 3H); ^{13}C NMR (125 MHz, DMSO-d_6): δ 164.72, 161.87, 159.76, 158.68, 156.38 (d, J_{C-F} = 255 Hz), 143.87, 136.99 (d, J_{C-F} = 10.00 Hz), 131.53, 130.91, 130.10, 124.63 (d, J_{C-F} = 2.50 Hz), 115.70, 115.64 (d, J_{C-F} = 13.75 Hz), 114.82 (d, J_{C-F} = 18.75 Hz), 68.64, 49.16, 18.44; ESI-HRMS: m/z calcd for $C_{20}H_{16}FN_7O_2S$ $[M+H]^+$ 438.1148, found 438.1149; HPLC: t_R = 7.36 min, flow rate 1.0 mL/min, COSMOSIL 5C18-MS-II column (4.6ID×250 mm), rt, eluent A-65%, eluent B-35%.

4-Amino-6-((1-(8-fluoro-1,1-dioxido-2-phenyl-2*H*-benzo[*e*][1,2,4]thiadiazin-3-yl)propyl)amino)pyrimidine-5-carbonitrile (**70**) White solid, yield 69%; ^{1}H NMR (500 MHz, DMSO-d_6): δ 7.92 (s, 1H), 7.90–7.83 (m, 1H), 7.57 (s, 5H), 7.54–7.48 (m, 2H), 7.43 (d, 8.0 Hz, 1H), 7.33 (brs, 2H), 4.59–4.52 (m, 1H), 1.94–1.84 (m, 2H), 0.76 (t, 7.5 Hz, 3H); ^{13}C NMR (125 MHz, DMSO-d_6): δ 164.71, 162.51, 159.81, 157.91, 156.30 (d, J_{C-F} = 255 Hz), 143.74, 136.03 (d, J_{C-F} = 10.0 Hz), 131.65, 130.96, 130.77, 130.18, 124.63 (d, J_{C-F} = 2.50 Hz), 115.76 (d, J_{C-F} = 13.75 Hz), 115.70, 114.97 (d, J_{C-F} = 20.00 Hz), 68.78, 54.53, 25.42, 10.93; ESI-HRMS: m/z calcd for $C_{21}H_{18}FN_7O_2S$ $[M+H]^+$ 452.1305, found

452.1318; HPLC: t_R = 10.23 min, flow rate 1.0 mL/min, COSMOSIL 5C18-MS-II column (4.6ID×250 mm), rt, eluent A-65%, eluent B-35%.

4-Amino-6-((1-(8-chloro-1,1-dioxido-2-phenyl-2*H*-benzo[*e*][1,2,4]thiadiazin-3-yl)ethyl)amino)pyrimidine-5-carbonitrile (**71**) White solid, yield 62%; ^{1}H NMR (500 MHz, DMSO-d_6): δ 7.91 (s, 1H), 7.76 (t, 8.0 Hz, 1H), 7.66–7.63 (m, 2H), 7.59–7.56 (m, 2H), 7.55–7.47 (m, 4H), 7.28 (brs, 2H), 4.69–4.56 (m, 1H), 1.38 (d, 6.5 Hz, 3H); ^{13}C NMR (125 MHz, DMSO-d_6): δ 164.71, 161.88, 159.76, 158.32, 144.10, 135.17, 131.84, 130.91, 130.86, 130.06, 129.79, 128.02, 127.95, 125.18, 115.71, 68.64, 49.13, 18.38; ESI-HRMS: m/z calcd for $C_{20}H_{16}ClN_7O_2S$ $[M+H]^+$ 454.0853, found 454.0850; HPLC: t_R = 10.09 min, flow rate 1.0 mL/min, COSMOSIL 5C18-MS-II column (4.6ID×250 mm), rt, eluent A-65%, eluent B-35%.

4-Amino-6-((1-(8-chloro-1,1-dioxido-2-phenyl-2*H*-benzo[*e*][1,2,4]thiadiazin-3-yl)propyl)amino)pyrimidine-5-carbonitrile (**72**) White solid; yield 71%; ^{1}H NMR (500 MHz, DMSO-d_6): δ 7.92 (s, 1H), 7.81 (t, 8.0 Hz, 1H), 7.69 (d, 7.5 Hz, 1H), 7.61–7.47 (m, 7H), 7.33 (brs, 2H), 4.59–4.49 (m, 1H), 1.93–1.81 (m, 2H), 0.76 (t, 7.0 Hz, 3H); ^{13}C NMR (125 MHz, DMSO-d_6): δ 164.70, 162.52, 159.81, 157.55, 143.98, 135.21, 131.97, 130.92, 130.78, 130.13, 129.91, 128.02, 127.91, 125.34, 115.71, 68.78, 54.47, 25.36, 10.90; ESI-HRMS: m/z calcd for $C_{21}H_{18}ClN_7O_2S$ $[M+H]^+$ 468.1009, found 468.1001; HPLC: t_R = 9.37 min, flow rate 1.0 mL/min, COSMOSIL 5C18-MS-II column (4.6ID×250 mm), rt, eluent A-70%, eluent B-30%.

*4.1.7. General procedure for target compounds **73-78***

To a solution of **32** (60 mg, 0.165 mmol, 1.0 eq) and adenine (22 mg, 0.165 mmol, 1.0 eq) in anhydrous DMF (1 mL) was added anhydrous K_2CO_3 (23 mg, 0.165 mmol, 1.0 eq). The resultant mixture was stirred at room temperature for 6 h, and H_2O was added under agitation to quench the reaction. After filtration, the solution of the filter cake in DCM was washed successively with H_2O and brine, dried over anhydrous Na_2SO_4, and concentrated in vacuo. The residue was subjected to flash column chromatography utilizing EA as the eluent to afford 3-(1-(6-amino-9*H*-purin-9-yl)ethyl)-2-phenyl-2*H*-benzo[*e*][1,2,4]thiadiazine 1,1-dioxide **73** as a white solid. Yield 65%; ^{1}H NMR (500 MHz, DMSO-d_6): δ 8.15 (s, 1H), 7.99–7.92 (m, 2H), 7.84 (t, 8.0 Hz, 1H), 7.64 (t, 7.5 Hz, 1H), 7.57 (d, 8.0 Hz, 1H), 7.53–7.42 (m, 3H), 7.34 (brs, 2H), 7.21 (s, 2H), 5.41 (q, 7.0 Hz, 1H), 1.78 (d, 7.0 Hz, 3H); ^{13}C NMR (100 MHz, DMSO-d_6): δ 158.28, 154.37, 152.84, 149.49, 141.45, 139.57, 135.01, 131.94, 130.74, 130.31, 129.60, 129.03, 128.72, 127.12, 121.99, 118.56, 51.26,

18.91; ESI-HRMS: m/z calcd for $C_{20}H_{17}N_7O_2S$ $[M+H]^+$ 420.1243, found 420.1243; HPLC: t_R = 7.11 min, flow rate 1.0 mL/min, COSMOSIL 5C18-MS-II column (4.6ID×250 mm), rt, eluent A-60%, eluent B-40%.

Compound **74-78** were prepared in a procedure similar to that described for **73**.

3-(1-(6-Amino-9*H*-purin-9-yl)ethyl)-2-(4-fluorophenyl)-2*H*-benzo[*e*][1,2,4]thiadiazine 1,1-dioxide (**74**) White solid; yield 47%; ^{1}H NMR (500 MHz, DMSO-d_6): δ 8.15 (s, 1H), 8.02–7.93 (m, 2H), 7.87 (t, 8.0 Hz, 1H), 7.75–7.53 (m, 3H), 7.45–7.07 (m, 5H), 5.44 (q, 7.0 Hz, 1H), 1.79 (d, 7.0 Hz, 3H); ^{13}C NMR (100 MHz, DMSO-d_6): δ 163.20 (d, J_{C-F} = 247 Hz), 156.30, 154.16, 152.82, 149.41, 141.42, 139.38, 135.07, 132.02 (d, J_{C-F} = 9.00 Hz), 129.06, 128.78, 128.01, 126.99, 122.05, 118.53, 117.24 (d, J_{C-F} = 22.0 Hz), 51.21, 19.01; ESI-HRMS: m/z calcd for $C_{20}H_{16}FN_7O_2S$ $[M+H]^+$ 438.1148, found 438.1155; HPLC: t_R = 7.99 min, flow rate 1.0 mL/min, COSMOSIL 5C18-MS-II column (4.6ID×250 mm), rt, eluent A-60%, eluent B-40%.

3-(1-(6-Amino-9*H*-purin-9-yl)propyl)-2-(4-fluorophenyl)-2*H*-benzo[*e*][1,2,4]thiadiazine 1,1-dioxide (**75**) White solid; yield 62%; ^{1}H NMR (500 MHz, DMSO-d_6): δ 8.20 (s, 1H), 8.02–7.93 (m, 2H), 7.89 (t, 7.5 Hz, 1H), 7.73–7.63 (m, 2H), 7.50–7.01 (m, 6H), 5.25 (dd, 5.0 Hz, 9.5 Hz, 1H), 2.43–2.34 (m, 1H), 2.31–2.21 (m, 1H), 0.74 (t, 7.0 Hz, 3H); ^{13}C NMR (100 MHz, DMSO-d_6): δ 163.20 (d, J_{C-F} = 247 Hz), 156.29, 153.48, 152.82, 149.95, 141.42, 139.56, 135.06, 132.01 (d, J_{C-F} = 8.00 Hz), 129.15, 128.84, 128.08 (d, J_{C-F} = 2.00 Hz), 127.13, 122.00, 118.31, 117.27 (d, J_{C-F} = 24.0 Hz), 56.43, 26.78, 10.75; ESI-HRMS: m/z calcd for $C_{21}H_{18}FN_7O_2S$ $[M+H]^+$ 452.1305, found 452.1303; HPLC: t_R = 11.06 min, flow rate 1.0 mL/min, COSMOSIL 5C18-MS-II column (4.6ID×250 mm), rt, eluent A-60%, eluent B-40%.

3-(1-(6-Amino-9*H*-purin-9-yl)propyl)-2-(4-(trifluoromethoxy)phenyl)-2*H*-benzo[*e*][1,2,4]thiadiazine 1,1-dioxide (**76**) White solid; yield 55%; ^{1}H NMR (500 MHz, DMSO-d_6): δ 8.15 (s, 1H), 7.98 (d, 7.5 Hz, 1H), 7.95–7.83 (m, 2H), 7.74 (d, 7.5 Hz, 1H), 7.69 (t, 7.0 Hz, 1H), 7.58–6.88 (m, 6H), 5.28 (t, 7.0 Hz, 1H), 2.45–2.35 (m, 1H), 2.32–2.19 (m, 1H), 0.74 (d, 7.0 Hz, 3H); ^{13}C NMR (100 MHz, DMSO-d_6): δ 156.31, 153.15, 152.78, 149.89, 149.62, 141.41, 139.30, 135.15, 131.61, 130.76, 129.30, 128.93, 127.22, 122.62, 121.99, 120.34 (q, J_{C-F} = 256 Hz), 118.23, 56.40, 26.85, 10.66; ESI-HRMS: m/z calcd for $C_{22}H_{18}F_3N_7O_3S$ $[M+H]^+$ 518.1222, found 518.1230; HPLC: t_R = 8.90 min, flow rate 1.0 mL/min, COSMOSIL 5C18-MS-II column (4.6ID×250 mm), rt, eluent A-70%, eluent B-30%.

3-(1-(6-Amino-9*H*-purin-9-yl)ethyl)-2-(pyridin-3-yl)-2*H*-benzo[*e*][1,2,4]thiadiazine 1,1-dioxide (**77**)

White solid; yield 52%; ^{1}H NMR (500 MHz, DMSO-d_6): δ 8.63 (d, 4.5 Hz, 1H), 8.47 (s, 1H), 8.14 (s, 1H), 7.99 (d, 7.5 Hz, 1H), 7.95 (s, 1H), 7.89 (t, 7.5 Hz, 1H), 7.76 (brs, 1H), 7.71–7.63 (m, 2H), 7.48 (brs, 1H), 7.25 (s, 2H), 5.46 (q, 6.5 Hz, 1H), 1.81 (d, 6.5 Hz, 3H); ^{13}C NMR (100 MHz, DMSO-d_6): δ 156.30, 153.70, 152.89, 151.37, 149.58, 149.32, 141.36, 139.25, 137.22, 135.23, 129.27, 129.15, 128.93, 127.00, 125.03, 122.06, 118.51, 51.29, 18.93; ESI-HRMS: m/z calcd for $C_{19}H_{16}N_8O_2S$ $[M+H]^+$ 421.1195, found 421.1195; HPLC: t_R = 9.61 min, flow rate 1.0 mL/min, COSMOSIL 5C18-MS-II column (4.6ID×250 mm), rt, eluent A-50%, eluent B-50%.

3-(1-(6-Amino-9*H*-purin-9-yl)ethyl)-8-fluoro-2-phenyl-2*H*-benzo[*e*][1,2,4]thiadiazine 1,1-dioxide (**78**) White solid; yield 48%; ^{1}H NMR (500 MHz, DMSO-d_6): δ 8.16 (s, 1H), 7.99 (s, 1H), 7.91–7.82 (m, 1H), 7.65–7.29 (m, 7H), 7.25 (s, 2H), 5.39 (q, 7.0 Hz, 1H), 1.78 (d, 7.0 Hz, 3H); ^{13}C NMR (100 MHz, DMSO-d_6): δ 156.27, 156.21 (d, $J_{C\text{-}F}$ = 255 Hz), 155.05, 152.85, 149.47, 143.25, 139.58, 136.12 (d, $J_{C\text{-}F}$ = 10.0 Hz), 131.10 (d, $J_{C\text{-}F}$ = 5.0 Hz), 130.35, 130.16, 125.10, 118.58, 115.79, 115.66, 115.61 (d, $J_{C\text{-}F}$ = 20.0 Hz), 51.39, 18.89; ESI-HRMS: m/z calcd for $C_{20}H_{16}FN_7O_2S$ $[M+H]^+$ 438.1148, found 438.1145; HPLC: t_R = 6.95 min, flow rate 1.0 mL/min, COSMOSIL 5C18-MS-II column (4.6ID×250 mm), rt, eluent A-60%, eluent B-40%.

*4.1.8. The procedure for optically pure compounds **S-63**, **R-63**, **S-71** and **R-71***

To a solution of **53** (1.00 g, 3.0 mmol, 1.0 eq) in EtOH (14 mL) was added a solution of *R*-mandelic acid (0.46 g, 3.0 mmol, 1.0eq) in EtOH (7 mL) dropwise at room temperature. The resultant mixture was stirred for 0.5 h, and white solid was precipitated during this period. Then, EA (7 mL) was added slowly, and the resultant mixture was allowed to stand at −10 °C for 4 h. After filtration, the filter cake was washed with pre-cooled EA, dried in vacuo, and subjected to recrystallization with EA to afford *R*-mandelic acid salt of ***S*-53** (*de* = 99 %) as the white crystal. Yield 34%; mp 173–175 °C; ESI-MS: m/z = 336 $[M+H]^+$; Chiral HPLC: t_R = 15.0 min, flow rate 0.5 mL/min, Welch Ultimate Cellud-Y column (4.6×250 mm, 5 μM), 15 °C, eluent C-40%, eluent D-60%.

The *S*-mandelic acid salt of ***R*-53** (*de* = 95 %) was obtained in a similar procedure to that for *R*-mandelic acid salt of ***S*-53** as the white crystal. Yield 42%; mp 174–175 °C; ESI-MS: m/z = 336 $[M+H]^+$; Chiral HPLC: t_R = 11.5 min, flow rate 0.5 mL/min, Welch Ultimate Cellud-Y column (4.6×250 mm, 5 μM), 15 °C, eluent C-40%, eluent D-60%.

The *S*-mandelic acid salt of ***R*-53** and *R*-mandelic acid salt of ***S*-53** were basified successively with NaOH solution (0.5 N) to afford ***R*-53** and ***S*-53**, respectively. The optical purity of ***R*-53** and ***S*-53** was

analyzed by chiral HPLC. ***R*-53**: *ee* = 95%; t_R = 11.5 min; ***S*-53**: *ee* = 99%; t_R = 15.0 min; Chiral HPLC: flow rate 0.5 mL/min, Welch Ultimate Cellud-Y column (4.6×250 mm, 5 μM), 15 ℃, eluent C-40%, eluent D-60%.

Compounds ***S-63***, ***R-63***, ***S-71*** *and* ***R-71*** were prepared in a procedure similar to that described for corresponding racemates.

(*S*)-3-(1-((9*H*-purin-6-yl)amino)ethyl)-8-chloro-2-phenyl-2*H*-benzo[*e*][1,2,4]thiadiazine 1,1-dioxide (***S*-63**) ^{1}H NMR (500 MHz, $CDCl_3$): δ 8.37 (s, 1H), 8.03 (s, 1H), 7.64–7.49 (m, 7H), 7.44 (dd, 1.0 Hz, 7.5 Hz, 1H), 7.00 (brs, 1H), 5.21–4.96 (m, 1H), 1.59 (d, 7.0 Hz, 3H); ESI-HRMS: m/z calcd for $C_{20}H_{16}ClN_7O_2S$ $[M+H]^+$ 454.0853, found 454.0840; HPLC: t_R = 9.16 min, flow rate 1.0 mL/min, COSMOSIL 5C18-MS-II column (4.6ID×250 mm), rt, eluent A-65%, eluent B-35%. The title compound can be obtained as single crystal by slow evaporation from a solution of the pure compound in a mixture of EtOH and EA at room temperature.

(*S*)-3-(1-((9*H*-purin-6-yl)amino)ethyl)-8-chloro-2-phenyl-2*H*-benzo[*e*][1,2,4]thiadiazine 1,1-dioxide (***R*-63**) ^{1}H NMR (500 MHz, $CDCl_3$): δ 8.36 (s, 1H), 8.03 (s, 1H), 7.63–7.49 (m, 7H), 7.44 (d, 7.5 Hz, 1H), 6.96 (brs, 1H), 5.19–4.98 (m, 1H), 1.59 (d, 6.5 Hz, 3H); ESI-HRMS: m/z calcd for $C_{20}H_{16}ClN_7O_2S$ $[M+H]^+$ 454.0853, found 454.0841; HPLC: t_R = 7.88 min, flow rate 1.2 mL/min, COSMOSIL 5C18-MS-II column (4.6ID×250 mm), rt, eluent A-65%, eluent B-35%.

(*S*)-4-amino-6-((1-(8-chloro-1,1-dioxido-2-phenyl-2H-benzo[*e*][1,2,4]thiadiazin-3-yl)ethyl)amino)pyrimidine-5-carbonitrile (***S*-71**) ^{1}H NMR (500 MHz, $CDCl_3$): δ 8.11 (s, 1H), 7.66–7.44 (m, 8H), 6.53 (d, 7.5 Hz, 1H), 5.47 (s, 2H), 4.96–4.86 (m, 1H), 1.49 (d, 7.0 Hz, 3H); ESI-HRMS: m/z calcd for $C_{20}H_{16}ClN_7O_2S$ $[M+H]^+$ 454.0853, found 454.0835; HPLC: t_R = 10.32 min, flow rate 1.0 mL/min, COSMOSIL 5C18-MS-II column (4.6ID×250 mm), rt, eluent A-65%, eluent B-35%.

(*R*)-4-amino-6-((1-(8-chloro-1,1-dioxido-2-phenyl-2H-benzo[*e*][1,2,4]thiadiazin-3-yl)ethyl)amino)pyrimidine-5-carbonitrile (***R*-71**) ^{1}H NMR (500 MHz, $CDCl_3$): δ 8.10 (s, 1H), 7.66–7.41 (m, 8H), 6.57 (d, 7.5 Hz, 1H), 5.56 (s, 2H), 4.95–4.86 (m, 1H), 1.49 (d, 6.5 Hz, 3H); ESI-HRMS: m/z calcd for $C_{20}H_{16}ClN_7O_2S$ $[M+H]^+$ 454.0853, found 454.0864; HPLC: t_R = 10.29 min, flow rate 1.0 mL/min, COSMOSIL 5C18-MS-II column (4.6ID×250 mm), rt, eluent A-65%, eluent B-35%.

4.2. Class I PI3Ks Biochemical Assay

ADP-Glo Luminescent Assay (Promega) was performed for evaluating the inhibitory activities

against PI3Kδ (Invitrogen), PI3Kβ (Millipore) and PI3K γ (Invitrogen), while Kinase-Glo Luminescent Assay (Promega) was performed for evaluating the inhibitory activity against PI3Kα (Invitrogen).

For PI3Kδ biochemical assay, the kinase was dissolved in the kinase buffer, containing 50 mM HEPES (pH 7.5), 3 mM $MgCl_2$, 1 mM EDTA, 100 mM NaCl, 0.03% CHAPS, and 2 mM DTT, to prepare the kinase solution, and PIP_2 and ATP were dissolved in the kinase buffer to prepare the substrate solution. Serially diluted compound solutions were added successively to the well of the 384-well assay plate (Corning). After the successive addition of the kinase solution and the substrate solution, the reaction mixture, with the final concentration of PI3Kδ being 2.4 nM, was incubated at room temperature for 2 h, and then stopped by ADP-Glo reagent. After being equilibrated, the mixture was treated with the kinase detection reagent. The plates were read in a Synergy reader for luminescence. The percent inhibition was calculated as (max−sample RLU)/(max−min)*100. Herein, 'min' stands for the RLU of no enzyme control, while 'max' means the RLU of DMSO control. PI3Kβ and γ inhibitory activities were evaluated according to the PI3Kδ inhibition assay with minor modification. The final concentrations of PI3Kβ and PI3Kγ in the kinase reaction mixture were 4.8 and 7.6 nM, respectively.

The composition of the kinase buffer, as well as the preparation of the kinase solution and the substrate solution, in PI3Kα inhibition assay was identical to those in PI3Kδ biochemical assay. The final concentration of PI3Kα in the kinase reaction mixture was 1.65 nM. After incubation at room temperature for 1 h, the kinase reaction was stopped by Kinase-Glo reagent. The plates were read in a Flexstation reader for luminescence. The percent inhibition was calculated as 100−(max−sample RLU)/(max−min)*100. Herein, 'max' stands for the RLU of no enzyme control, while 'min' means the RLU of DMSO control. Finally, all the collected data were presented in MS Excel and the curves fitted by Graphpad 5.0 for identifying IC_{50} values.

4.3. Anti-proliferative Assay

CellTiter-Glo luminescent cell viability assay purchased from Promega was performed to evaluate the anti-proliferative activity against SU-DHL-6 cell line (ATCC). Cells were seeded in 96-well plates (Costar) at the density of 1×10^4 cells per well, and co-incubated with the tested compounds or the medium alone at the indicated concentrations for 72 h. Cell lysis was induced by the addition of 30 μL CellTiter-Glo reagent. After equilibration, an appropriate amount of the mixture from each well was

transferred to a new 96-well black plate and the luminescence was read on EnSpire. The collected data were analyzed by XLFit software to give GI_{50} values.

4.4. PK Evaluation

The PK profiles of ***S*-63** and idelalisib were tested in three male SD rats dosed iv (2 mg/kg) and orally (10 mg/kg), respectively. The intravenous dose was formulated in a solution of 5% DMSO, 10% Solutol, 10% EtOH and 75% Saline at 0.4 mg/mL, while the oral dose was formulated in a homogenous opaque suspension of 2%DMSO and 98% MC (0.5%) at 1 mg/mL. At the designated time points, the animal was anaesthetized with isoflurane and blood sample was collected *via* orbit for terminal bleeding into EDTA-2K tubes. Terfenadine and buspirone (10.0 ng/mL) in CH_3CN was used as the internal standard for the PK study of ***S*-63**, while terfenadine and buspirone (50.0 ng/mL) in CH_3CN was used as the internal standard for the PK study of idelalisib. The plasma samples were stored at –20℃ until the analysis and the concentration of the tested compound in plasma was determined with LC/MS/MS.

4.5. Molecular docking

The co-crystal structure of PI3Kδ complexed with idelalisib (PDB code 4XE0) [29] was used for the molecular docking analysis in C-DOCKER module of Discovery Studio (version 2.5; Accelrys, San Diego, CA, USA, 2008). The 3D structures of the ligands were generated and the energy minimization was performed. CHARMm-force field was applied to the protein after removing idelalisib and solvent molecules. The active site of the receptor was determined according to the location of idelalisib in PI3Kδ and each ligand was docked into the defined site. The final binding conformations of them were determined on the basis of the calculated C-DOCKING ENERGE.

Conflict of interest

The authors confirm that this article content has no conflicts of interest.

References

[1] V. S. Rodrik-Outmezguine; M. Okaniwa; Z. Yao; C. J. Novotny; C. McWhirter; A. Banaji; H. Won; W. Wong; M. Berger; E. de Stanchina; D. G. Barratt; S. Cosulich; T. Klinowska; N. Rosen; K. M.

Shokat, Overcoming mTOR resistance mutations with a new-generation mTOR inhibitor. *Nature* **2016,** *534* (7606), 272-276.

[2] T. P. Heffron; R. A. Heald; C. Ndubaku; B. Wei; M. Augistin; S. Do; K. Edgar; C. Eigenbrot; L. Friedman; E. Gancia; P. S. Jackson; G. Jones; A. Kolesnikov; L. B. Lee; J. D. Lesnick; C. Lewis; N. McLean; M. Mortl; J. Nonomiya; J. Pang; S. Price; W. W. Prior; L. Salphati; S. Sideris; S. T. Staben; S. Steinbacher; V. Tsui; J. Wallin; D. Sampath; A. G. Olivero, The Rational Design of Selective Benzoxazepin Inhibitors of the alpha-Isoform of Phosphoinositide 3-Kinase Culminating in the Identification of (S)-2-((2-(1-Isopropyl-1H-1,2,4-triazol-5-yl)-5,6-dihydrobenzo[f]imidazo[1,2-d][1 ,4]oxazepin-9-yl)oxy)propanamide (GDC-0326). *J Med Chem* **2016,** *59* (3), 985-1002.

[3] F. Gonzalez-Lopez de Turiso; Y. Shin; M. Brown; M. Cardozo; Y. Chen; D. Fong; X. Hao; X. He; K. Henne; Y. L. Hu; M. G. Johnson; T. Kohn; J. Lohman; H. J. McBride; L. R. McGee; J. C. Medina; D. Metz; K. Miner; D. Mohn; V. Pattaropong; J. Seganish; J. L. Simard; S. Wannberg; D. A. Whittington; G. Yu; T. D. Cushing, Discovery and in vivo evaluation of dual PI3Kbeta/delta inhibitors. *J Med Chem* **2012,** *55* (17), 7667-7685.

[4] M. Erra; J. Taltavull; A. Greco; F. J. Bernal; J. F. Caturla; J. Gracia; M. Dominguez; M. Sabate; S. Paris; S. Soria; B. Hernandez; C. Armengol; J. Cabedo; M. Bravo; E. Calama; M. Miralpeix; M. D. Lehner, Discovery of a Potent, Selective, and Orally Available PI3Kdelta Inhibitor for the Treatment of Inflammatory Diseases. *ACS Med Chem Lett* **2017,** *8* (1), 118-123.

[5] A. Amour; N. Barton; A. W. Cooper; G. Inglis; C. Jamieson; C. N. Luscombe; J. Morrell; S. Peace; D. Perez; P. Rowland; C. J. Tame; S. Uddin; G. Vitulli; N. Wellaway, Evolution of a Novel, Orally Bioavailable Series of PI3Kdelta Inhibitors from an Inhaled Lead for the Treatment of Respiratory Disease. *J Med Chem* **2016,** *59* (15), 7239-7251.

[6] D. A. Fruman; C. Rommel, PI3K and cancer: lessons, challenges and opportunities. *Nat Rev Drug Discov* **2014,** *13* (2), 140-156.

[7] P. J. Parker, The ubiquitous phosphoinositides. *Biochem Soc Trans* **2004,** *32* (Pt 6), 893-898.

[8] M. Elkabets; S. Vora; D. Juric; N. Morse; M. Mino-Kenudson; T. Muranen; J. Tao; A. B. Campos; J. Rodon; Y. H. Ibrahim; V. Serra; V. Rodrik-Outmezguine; S. Hazra; S. Singh; P. Kim; C. Quadt; M. Liu; A. Huang; N. Rosen; J. A. Engelman; M. Scaltriti; J. Baselga, mTORC1 inhibition is required for sensitivity to PI3K p110alpha inhibitors in PIK3CA-mutant breast cancer. *Sci Transl*

Med **2013,** *5* (196), 196ra199.

[9] X. Ma; Y. Hu, Targeting PI3K/Akt/mTOR cascade: the medicinal potential, updated research highlights and challenges ahead. *Curr Med Chem* **2013,** *20* (24), 2991-3010.

[10] S. A. Meadows; F. Vega; A. Kashishian; D. Johnson; V. Diehl; L. L. Miller; A. Younes; B. J. Lannutti, PI3Kdelta inhibitor, GS-1101 (CAL-101), attenuates pathway signaling, induces apoptosis, and overcomes signals from the microenvironment in cellular models of Hodgkin lymphoma. *Blood* **2012,** *119* (8), 1897-1900.

[11] B. J. Lannutti; S. A. Meadows; S. E. Herman; A. Kashishian; B. Steiner; A. J. Johnson; J. C. Byrd; J. W. Tyner; M. M. Loriaux; M. Deininger; B. J. Druker; K. D. Puri; R. G. Ulrich; N. A. Giese, CAL-101, a p110delta selective phosphatidylinositol-3-kinase inhibitor for the treatment of B-cell malignancies, inhibits PI3K signaling and cellular viability. *Blood* **2011,** *117* (2), 591-594.

[12] T. D. Cushing; D. P. Metz; D. A. Whittington; L. R. McGee, PI3Kdelta and PI3Kgamma as targets for autoimmune and inflammatory diseases. *J Med Chem* **2012,** *55* (20), 8559-8581.

[13] Y. Shin; J. Suchomel; M. Cardozo; J. Duquette; X. He; K. Henne; Y. L. Hu; R. C. Kelly; J. McCarter; L. R. McGee; J. C. Medina; D. Metz; T. San Miguel; D. Mohn; T. Tran; C. Vissinga; S. Wong; S. Wannberg; D. A. Whittington; J. Whoriskey; G. Yu; L. Zalameda; X. Zhang; T. D. Cushing, Discovery, Optimization, and in Vivo Evaluation of Benzimidazole Derivatives AM-8508 and AM-9635 as Potent and Selective PI3Kdelta Inhibitors. *J Med Chem* **2016,** *59* (1), 431-447.

[14] M. Thomas; C. Owen, Inhibition of PI-3 kinase for treating respiratory disease: good idea or bad idea? *Curr Opin Pharmacol* **2008,** *8* (3), 267-274.

[15] B. Barlaam; S. Cosulich; S. Degorce; M. Fitzek; S. Green; U. Hancox; C. Lambert-van der Brempt; J. J. Lohmann; M. Maudet; R. Morgentin; M. J. Pasquet; A. Peru; P. Ple; T. Saleh; M. Vautier; M. Walker; L. Ward; N. Warin, Discovery of (R)-8-(1-(3,5-difluorophenylamino)ethyl)-N,N-dimethyl-2-morpholino-4-oxo-4H-chrom ene-6-carboxamide (AZD8186): a potent and selective inhibitor of PI3Kbeta and PI3Kdelta for the treatment of PTEN-deficient cancers. *J Med Chem* **2015,** *58* (2), 943-962.

[16] B. S. Safina; S. Baker; M. Baumgardner; P. M. Blaney; B. K. Chan; Y. H. Chen; M. W. Cartwright; G. Castanedo; C. Chabot; A. J. Cheguillaume; P. Goldsmith; D. M. Goldstein; B. Goyal; T. Hancox; R. K. Handa; P. S. Iyer; J. Kaur; R. Kondru; J. R. Kenny; S. L. Krintel; J. Li; J. Lesnick;

M. C. Lucas; C. Lewis; S. Mukadam; J. Murray; A. J. Nadin; J. Nonomiya; F. Padilla; W. S. Palmer; J. Pang; N. Pegg; S. Price; K. Reif; L. Salphati; P. A. Savy; E. M. Seward; S. Shuttleworth; S. Sohal; Z. K. Sweeney; S. Tay; P. Tivitmahaisoon; B. Waszkowycz; B. Wei; Q. Yue; C. Zhang; D. P. Sutherlin, Discovery of novel PI3-kinase delta specific inhibitors for the treatment of rheumatoid arthritis: taming CYP3A4 time-dependent inhibition. *J Med Chem* **2012,** *55* (12), 5887-5900.

[17] J. M. Murray; Z. K. Sweeney; B. K. Chan; M. Balazs; E. Bradley; G. Castanedo; C. Chabot; D. Chantry; M. Flagella; D. M. Goldstein; R. Kondru; J. Lesnick; J. Li; M. C. Lucas; J. Nonomiya; J. Pang; S. Price; L. Salphati; B. Safina; P. P. Savy; E. M. Seward; M. Ultsch; D. P. Sutherlin, Potent and highly selective benzimidazole inhibitors of PI3-kinase delta. *J Med Chem* **2012,** *55* (17), 7686-7695.

[18] S. Perreault; J. Chandrasekhar; Z. H. Cui; J. Evarts; J. Hao; J. A. Kaplan; A. Kashishian; K. S. Keegan; T. Kenney; D. Koditek; L. Lad; E. I. Lepist; M. E. McGrath; L. Patel; B. Phillips; J. Therrien; J. Treiberg; A. Yahiaoui; G. Phillips, Discovery of a Phosphoinositide 3-Kinase (PI3K) beta/delta Inhibitor for the Treatment of Phosphatase and Tensin Homolog (PTEN) Deficient Tumors: Building PI3Kbeta Potency in a PI3Kdelta-Selective Template by Targeting Nonconserved Asp856. *J Med Chem* **2017,** *60* (4), 1555-1567.

[19] C. Xie; Y. He; M. Zhen; Y. Wang; Y. Xu; L. Lou, Puquitinib, a novel orally available PI3Kdelta inhibitor, exhibits potent antitumor efficacy against acute myeloid leukemia. *Cancer Sci* **2017,** *108* (7), 1476-1484.

[20] L. Patel; J. Chandrasekhar; J. Evarts; A. C. Haran; C. Ip; J. A. Kaplan; M. Kim; D. Koditek; L. Lad; E. I. Lepist; M. E. McGrath; N. Novikov; S. Perreault; K. D. Puri; J. R. Somoza; B. H. Steiner; K. L. Stevens; J. Therrien; J. Treiberg; A. G. Villasenor; A. Yeung; G. Phillips, 2,4,6-Triaminopyrimidine as a Novel Hinge Binder in a Series of PI3Kdelta Selective Inhibitors. *J Med Chem* **2016,** *59* (7), 3532-3548.

[21] F. Gonzalez-Lopez de Turiso; X. Hao; Y. Shin; M. Bui; I. D. Campuzano; M. Cardozo; M. C. Dunn; J. Duquette; B. Fisher; R. S. Foti; K. Henne; X. He; Y. L. Hu; R. C. Kelly; M. G. Johnson; B. S. Lucas; J. McCarter; L. R. McGee; J. C. Medina; D. Metz; T. San Miguel; D. Mohn; T. Tran; C. Vissinga; S. Wannberg; D. A. Whittington; J. Whoriskey; G. Yu; L. Zalameda; X. Zhang; T. D. Cushing, Discovery and in Vivo Evaluation of the Potent and Selective PI3Kdelta Inhibitors

2-((1S)-1-((6-Amino-5-cyano-4-pyrimidinyl)amino)ethyl)-6-fluoro-N-methyl-3-(2-pyridinyl)-4-quinolinecarboxamide (AM-0687) and 2-((1S)-1-((6-Amino-5-cyano-4-pyrimidinyl)amino)ethyl)-5-fluoro-N-methyl-3-(2-pyridinyl)-4-quinolinecarboxamide (AM-1430). *J Med Chem* **2016,** *59* (15), 7252-7267.

[22] K. Down; A. Amour; I. R. Baldwin; A. W. Cooper; A. M. Deakin; L. M. Felton; S. B. Guntrip; C. Hardy; Z. A. Harrison; K. L. Jones; P. Jones; S. E. Keeling; J. Le; S. Livia; F. Lucas; C. J. Lunniss; N. J. Parr; E. Robinson; P. Rowland; S. Smith; D. A. Thomas; G. Vitulli; Y. Washio; J. N. Hamblin, Optimization of Novel Indazoles as Highly Potent and Selective Inhibitors of Phosphoinositide 3-Kinase delta for the Treatment of Respiratory Disease. *J Med Chem* **2015,** *58* (18), 7381-7399.

[23] C. C. Ma; C. M. Zhang; L. Q. Tang; Z. P. Liu, Discovery of novel quinazolinone derivatives as high potent and selective PI3Kdelta and PI3Kdelta/gamma inhibitors. *Eur J Med Chem* **2018,** *151*, 9-17.

[24] M. Wei; X. Zhang; X. Wang; Z. Song; J. Ding; L. H. Meng; A. Zhang, SAR study of 5-alkynyl substituted quinazolin-4(3H)-ones as phosphoinositide 3-kinase delta (PI3Kdelta) inhibitors. *Eur J Med Chem* **2017,** *125*, 1156-1171.

[25] R. Dienstmann; J. Rodon; V. Serra; J. Tabernero, Picking the point of inhibition: a comparative review of PI3K/AKT/mTOR pathway inhibitors. *Mol Cancer Ther* **2014,** *13* (5), 1021-1031.

[26] Q. Yang; P. Modi; T. Newcomb; C. Queva; V. Gandhi, Idelalisib: First-in-Class PI3K Delta Inhibitor for the Treatment of Chronic Lymphocytic Leukemia, Small Lymphocytic Leukemia, and Follicular Lymphoma. *Clin Cancer Res* **2015,** *21* (7), 1537-1542.

[27] D. G. Winkler; K. L. Faia; J. P. DiNitto; J. A. Ali; K. F. White; E. E. Brophy; M. M. Pink; J. L. Proctor; J. Lussier; C. M. Martin; J. G. Hoyt; B. Tillotson; E. L. Murphy; A. R. Lim; B. D. Thomas; J. R. Macdougall; P. Ren; Y. Liu; L. S. Li; K. A. Jessen; C. C. Fritz; J. L. Dunbar; J. R. Porter; C. Rommel; V. J. Palombella; P. S. Changelian; J. L. Kutok, PI3K-delta and PI3K-gamma inhibition by IPI-145 abrogates immune responses and suppresses activity in autoimmune and inflammatory disease models. *Chem Biol* **2013,** *20* (11), 1364-1374.

[28] A. Berndt; S. Miller; O. Williams; D. D. Le; B. T. Houseman; J. I. Pacold; F. Gorrec; W. C. Hon; Y. Liu; C. Rommel; P. Gaillard; T. Ruckle; M. K. Schwarz; K. M. Shokat; J. P. Shaw; R. L. Williams, The p110 delta structure: mechanisms for selectivity and potency of new PI(3)K inhibitors. *Nat Chem Biol* **2010,** *6* (2), 117-124.

[29] J. R. Somoza; D. Koditek; A. G. Villasenor; N. Novikov; M. H. Wong; A. Liclican; W. Xing; L. Lagpacan; R. Wang; B. E. Schultz; G. A. Papalia; D. Samuel; L. Lad; M. E. McGrath, Structural, biochemical, and biophysical characterization of idelalisib binding to phosphoinositide 3-kinase delta. *J Biol Chem* **2015,** *290* (13), 8439-8446.

[30] P. Norman, Selective PI3Kdelta inhibitors, a review of the patent literature. *Expert Opin Ther Pat* **2011,** *21* (11), 1773-1790.

[31] M. W. D. Perry; R. Abdulai; M. Mogemark; J. Petersen; M. J. Thomas; B. Valastro; A. W. Eriksson, Evolution of PI3Kγ and δ Inhibitors for Inflammatory and Autoimmune Diseases. *J Med Chem* **2019,** doi: 10.1021/acs.jmedchem.8b01298.

[32] S. Zhersh; O. Lukin; V. Matvienko; A. Tolmachev, Synthesis of isomeric fluoronitrobenzene-sulfonyl chlorides. *Tetrahedron* **2010,** *66*, 5982-5986.

[33] C. V. Kumar; K. R. Gopidas; K. Bhattacharyya; P. K. Das; M. V. George, Photoinduced Ring Enlargement Reactions of 2*H*- l,2,4-Benzothiadiazine 1,l-Dioxides. Steady-State and Laser Flash Photolysis Studies. *J Org Chem* **1986,** *51* (11), 1967-1972.

[34] S. A. Brunton; J. H. Stibbard; L. L. Rubin; L. I. Kruse; O. M. Guicherit; E. A. Boyd; S. Price, Potent inhibitors of the hedgehog signaling pathway. *J Med Chem* **2008,** *51* (5), 1108-1110.

[35] Y. C. Chen; X. Y. Zeng; Y. He; H. Liu; B. Wang; H. Zhou; J. W. Chen; P. Q. Liu; L. Q. Gu; J. M. Ye; Z. S. Huang, Rutaecarpine analogues reduce lipid accumulation in adipocytes via inhibiting adipogenesis/lipogenesis with AMPK activation and UPR suppression. *ACS Chem Biol* **2013,** *8* (10), 2301-2311.

[36] T. D. Cushing; X. Hao; Y. Shin; K. Andrews; M. Brown; M. Cardozo; Y. Chen; J. Duquette; B. Fisher; F. Gonzalez-Lopez de Turiso; X. He; K. R. Henne; Y. L. Hu; R. Hungate; M. G. Johnson; R. C. Kelly; B. Lucas; J. D. McCarter; L. R. McGee; J. C. Medina; T. San Miguel; D. Mohn; V. Pattaropong; L. H. Pettus; A. Reichelt; R. M. Rzasa; J. Seganish; A. S. Tasker; R. C. Wahl; S. Wannberg; D. A. Whittington; J. Whoriskey; G. Yu; L. Zalameda; D. Zhang; D. P. Metz, Discovery and in vivo evaluation of (S)-N-(1-(7-fluoro-2-(pyridin-2-yl)quinolin-3-yl)ethyl)-9H-purin-6-amine (AMG319) and related PI3Kdelta inhibitors for inflammation and autoimmune disease. *J Med Chem* **2015,** *58* (1), 480-511.

Highlights

- 24 benzothiadiazine derivatives with structural novelty were designed, synthesized and biologically evaluated as PI3Kδ-selective inhibitors.
- Chiral resolution of the key amine intermediate of representative compounds **63** and **71** was performed to achieve corresponding enantiomers.
- ***S*-63** and ***S*-71** exhibited remarkable PI3Kδ inhibitory activity, potent anti-proliferative efficacy against human malignant B-cell line SU-DHL-6, and excellent PI3Kδ selectivity.
- ***S*-63** displayed a good plasma exposure and an acceptable oral bioavailability of 29.2%.